

INFLUENCE OF FATIGUE LOADS ON THE LAXITY  
OF LUMBAR INTERVERTEBRAL JOINTS

By

ENOCH MYLABATHULA

Bachelor of Technology

Jawaharlal Nehru Technological University

Kakinada, Andhra Pradesh, India.

1983

Submitted to the Faculty of the  
Graduate College of the  
Oklahoma State University  
in partial fulfillment of  
the requirements for  
the Degree of  
MASTER OF SCIENCE  
December, 1987

Thesis  
1987  
M997i  
cop. 2



INFLUENCE OF FATIGUE LOADS ON THE LAXITY  
OF LUMBAR INTERVERTEBRAL JOINTS

Thesis Approved:

*Atmaram H. Sam-*

Thesis Adviser

*J. F. Reed*

*B. F. Lowery*

*Norman N. Durham*

Dean of the Graduate College

## PREFACE

I would like to express my sincere thanks and appreciation to my advisor Dr. Atmaram H. Soni for his original idea, guidance and support, which was the backbone for the success of this study.

My heartfelt thanks are due to Ram Gudavalli for his cooperation, constructive help and constant encouragement throughout the course of the study.

Special thanks are extended to Mike Jackson for his creative help in the fabrication of the fixtures.

Finally, I thank my father for his prayers, continual support and encouragement.

## TABLE OF CONTENTS

Chapter	Page
I. INTRODUCTION . . . . .	1
Biomechanical Anatomy of the Spine . . . . .	2
Prime Functions of the Spine. . . . .	5
Vertebra. . . . .	6
Intervertebral Disc . . . . .	6
Nucleus Pulposus . . . . .	6
Annulus Fibrosis . . . . .	7
Cartilaginous End Plate. . . . .	7
Hysteresis . . . . .	9
Loads Imposed on Spinal Column . . . . .	10
Bending . . . . .	10
Torsion . . . . .	12
Fatigue, its Effects and Importance. . . . .	12
II. PROPOSED RESEARCH . . . . .	15
III. FATIGUE TESTING APPARATUS . . . . .	16
Load Applying Mechanism. . . . .	16
Fixtures to Hold the Vertebra. . . . .	19
Compressive Preload Arrangement. . . . .	19
Cyclic Load Attachment . . . . .	21
Bending . . . . .	21
Torsion . . . . .	21
Load Measuring Setup . . . . .	23
Calibration of Gages. . . . .	26
IV. KINEMATICS OF SPINE . . . . .	29
Degrees of Freedom , . . . . .	29
Representation of 3-D Displacement . . . . .	30
Motion Segment . . . . .	32
Physiological Patterns of Motion . . . . .	32
V. MATERIALS AND METHOD. . . . .	34
Specimen Preparation . . . . .	34
Specimen Mounting. . . . .	34
Mobility Test. . . . .	36

Chapter	Page
VI. DATA ANALYSIS AND CONCLUSIONS . . . . .	41
Experiment I . . . . .	42
Results . . . . .	42
Experiment II. . . . .	45
Results . . . . .	46
Experiment III . . . . .	48
Results . . . . .	49
Conclusions and Recommendations. . . . .	51
Future Scope. . . . .	52
BIBLIOGRAPHY . . . . .	83
APPENDIX . . . . .	85

LIST OF TABLES

Table	Page
I. Summary of Loads Applied on the Motion Segment. . . . .	39

## LIST OF FIGURES

Figure	Page
1. Anatomy of Human Spine. . . . .	3
2. Anatomical Terminology. . . . .	4
3. Anatomy of the Disc and the Vertebra. . . . .	7
4. Estimation of Lumbar Trunk Loads. . . . .	11
5. Load Applying Mechanism . . . . .	18
6. Fixtures for Bending Fatigue Test . . . . .	21
7. Fixtures for Torsional Fatigue Test . . . . .	22
8. Basic Load Measuring Setup. . . . .	24
9. Calibration Curve for Bending Load Measurement. . .	27
10. Calibration Curve for Torsional Load Measurement. .	28
11. Screw Axis Representation . . . . .	31
12. Physiological Patterns of Motion. . . . .	33
13. Fixture for Mobility Test . . . . .	37
14. Loads Applied on the Motion Segment . . . . .	40
15. Variation of Bending Load . . . . .	43
16. Rotations for Different Loads (0 deg.) Under Torsional Fatigue Load. . . . .	53
17. Translations for Different Loads (0 deg.) Under Torsional Fatigue Load. . . . .	54
18. Rotations Under Positive Shear (0 deg.) Under Torsional Fatigue Load. . . . .	55
19. Rotations Under Negative Shear (0 deg.) Under Torsional Fatigue Load. . . . .	56



Figure	Page
20. Rotations Under Positive Moment (0 deg.) Under Torsional Fatigue Load. . . . .	57
21. Rotations Under Negative Moment (0 deg.) Under Torsional Fatigue Load. . . . .	58
22. Rotations Under Positive Torque Under Torsional Fatigue Load. . . . .	59
23. Rotations Under Negative Torque Under Torsional Fatigue Load. . . . .	60
24. Rotations for Different Loads (90 deg.) Under Torsional Fatigue Load. . . . .	61
25. Translations for Different Loads (90 deg.) Under Torsional Fatigue Load. . . . .	62
26. Rotations Under Positive Shear (90 deg.) Under Torsional Fatigue Load. . . . .	63
27. Rotations Under Negative Shear (90 deg.) Under Torsional Fatigue Load. . . . .	64
28. Rotations Under Positive Moment (90 deg.) Under Torsional Fatigue Load. . . . .	65
29. Rotations Under Negative Moment (90 deg.) Under Torsional Fatigue Load. . . . .	66
30. Points of Intersection of the Screw Axis With XY Plane for PT and NT Loads Under Torsional Fatigue Load. . . . .	67
31. Rotations for Different Loads (0 deg.) Under Bending Fatigue Load. . . . .	68
32. Translations for Different Loads (0 deg.) Under Bending Fatigue Load. . . . .	69
33. Rotations Under Positive Shear (0 deg.) Under Bending Fatigue Load. . . . .	70
34. Rotations Under Negative Shear (0 deg.) Under Bending Fatigue Load. . . . .	71
35. Rotations Under Positive Moment (0 deg.) Under Bending Fatigue Load. . . . .	72
36. Rotations Under Negative Moment (0 deg.) Under Bending Fatigue Load. . . . .	73

Figure	Page
37. Rotations Under Positive Torque Under Bending Fatigue Load. . . . .	74
38. Rotations Under Negative Torque Under Bending Fatigue Load. . . . .	75
39. Rotations for Different Loads (90 deg.) Under Bending Fatigue Load. . . . .	76
40. Translations for Different Loads (90 deg.) Under Bending Fatigue Load. . . . .	77
41. Rotations Under Positive Shear (90 deg.) Under Bending Fatigue Load. . . . .	78
42. Rotations Under Negative Shear (90 deg.) Under Bending Fatigue Load. . . . .	79
43. Rotations Under Positive Moment (90 deg.) Under Bending Fatigue Load. . . . .	80
44. Rotations Under Negative Moment (90 deg.) Under Bending Fatigue Load. . . . .	81
45. Points of Intersection of the Screw Axis With XY Plane for PT and NT Loads Under Bending Fatigue Load. . . . .	82

## CHAPTER I

### INTRODUCTION

Spine is a mechanical structure. The vertebrae articulate with each other in a controlled manner through a complex system of joints, ligaments and levers. The spine structure is designed in such a way as to protect the centrally located spinal cord. Research studies on human spine hold the key in comprehending many disorders like low back pain, scoliosis, clinical instability etc. Studies show that 80 percent of the human population complain about low back pain at some point in their lives. Statistics indicate that the most common cause for not reporting to work is low back pain. The costs of treatment and compensation for those suffering from back pain are estimated at 14 billion dollars a year. Low back pain has known to be taking its toll on active workers in the industry as well as sedentary workers in the office.

The prime cause for low back disorders is still an area to be explored. A detailed study including testing of cadavers in the laboratory, clinical studies on patients and theoretical analogies are necessary to aid in understanding the spine disorders. The intervertebral joint motion is considered to be important in the diagnosis and treatment

of many spinal disorders. Loading due to chronic occupational activity is a common load exerted on the spinal column. When the rate of damage due to chronic cyclic loading exceeds the rate of repair by the cellular mechanisms, serious disorders result in the spinal area of the body.

### Biomechanical Anatomy of the Spine

The normal spine is composed of 33 vertebrae separated by intervertebral discs. Basically a spine is divided into five regions (Figure 1).

The Cervical region consists of 7 vertebrae numbered C1 to C7.

The Thoracic region consists of 12 vertebrae numbered T1 to T12.

The Lumbar region consists of 5 vertebrae numbered L1 to L5.

The Sacral region consists of 5 vertebrae.

The Coccygeal region consists of 4 vertebrae.

The Sacral and Coccygeal regions are fused and the combined region is termed as sacrum.

Kyphosis and Lordosis are used to describe the curvatures in the Sagittal plane.

Sagittal plane is defined as that plane which divides the left side of the body from the right side.

The plane perpendicular to the Sagittal plane is called the Frontal plane (Figure 2).

As viewed in the Frontal plane, the spine generally appears straight and symmetrical. In some individuals there may be a slight right thoracic curve which may be due to

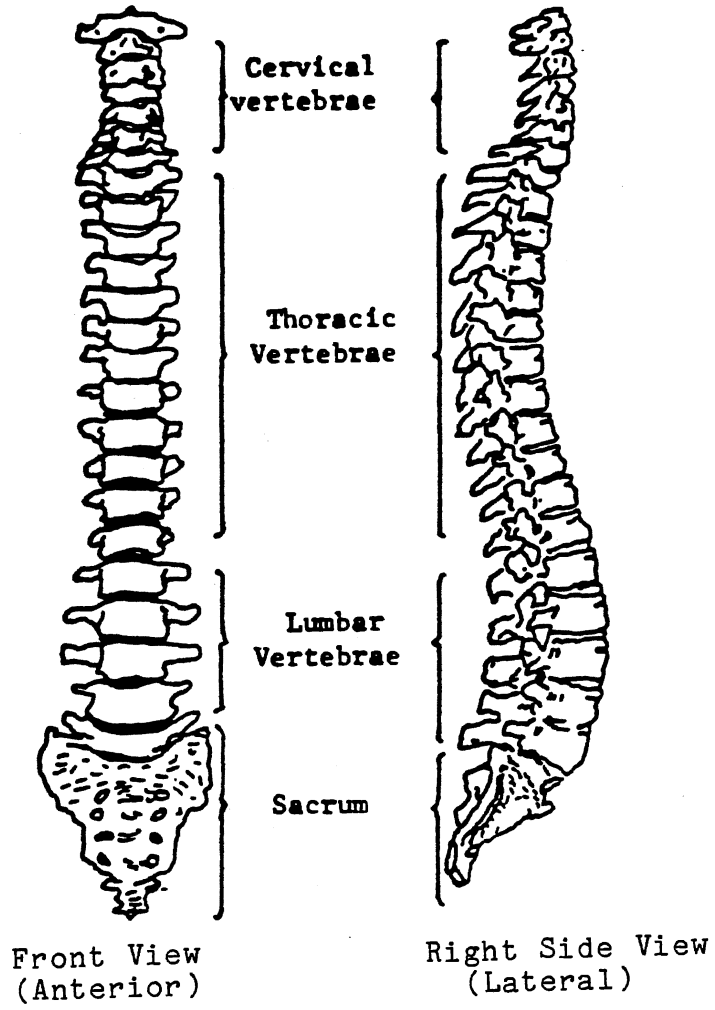


Figure 1. Anatomy of Human Spine

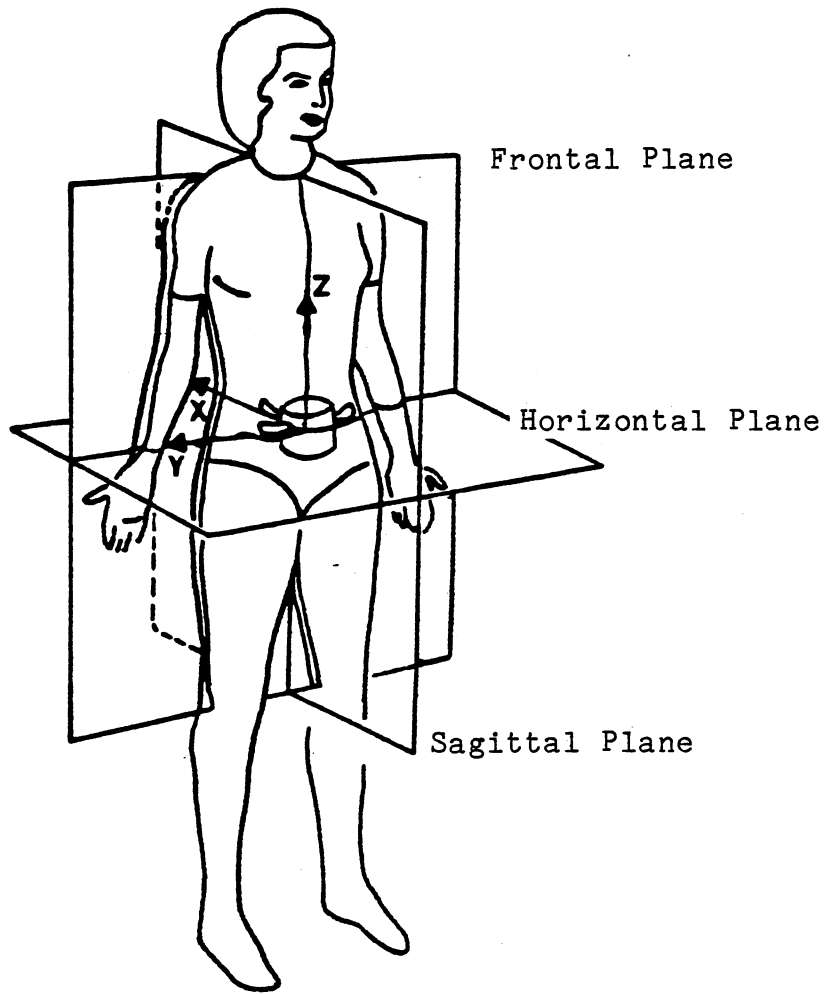


Figure 2. Anatomical Terminology

either the position of the aorta or to the increased use of the right hand. In the lateral or sagittal plane there are four normal curves. These curves are convex anteriorly in the cervical and the lumbar regions and convex posteriorly in the thoracic and sacral regions. There is a mechanical basis for these normal anatomic curves: they give the spinal column increased flexibility and augmented shock-absorbing capacity while at the same time maintaining adequate stiffness and stability at the intervertebral joint level. The thoracic curve is structural and is due to the lesser vertical height of the anterior thoracic vertebral borders, as opposed to the posterior. This is also true of the sacral curve. Curvature of the cervical and lumbar regions is largely due to the wedge shaped intervertebral discs. Consequently, when distracting forces are applied to the entire spine, there is a greater flattening of the cervical and lumbar lordosis as compared to the thoracic kyphosis.

#### Prime Functions of the Spine

- a. To transfer the weights and the bending moments of the head and trunk to the pelvis.
- b. To allow sufficient physiological motion between the head, trunk and pelvis.
- c. To protect the spinal cord from possible damage.

### Vertebra

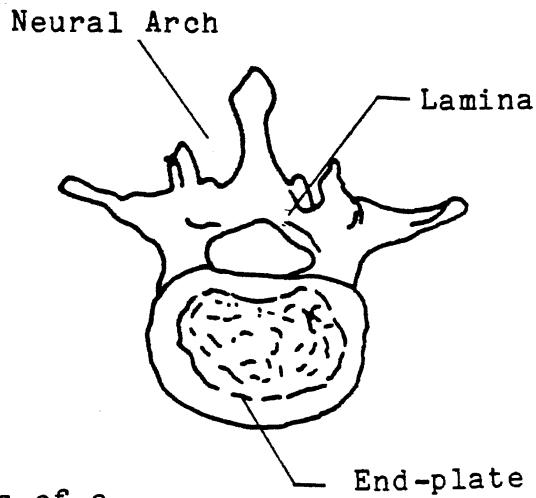
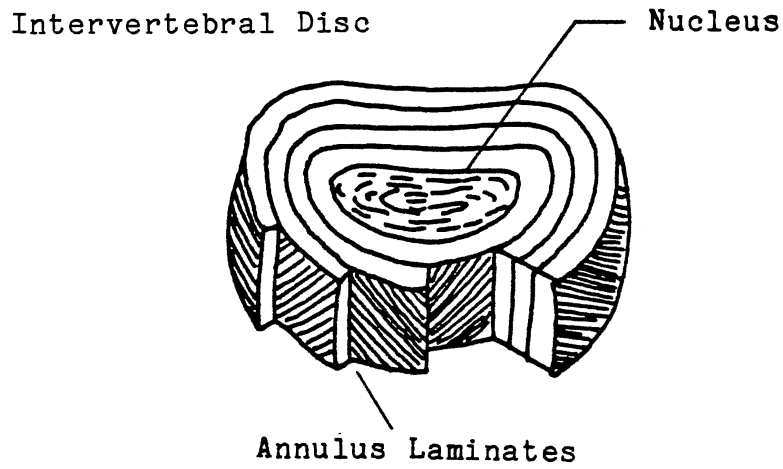
A vertebra consists of an anterior block of bone, the body and a posterior bony ring, known as the neural arch. The vertebral body is a roughly cylindrical mass of cancellous bone. Its top and bottom surfaces, slightly concave, are the vertebral end-plates. The neural arch comprises of two pedicles and two laminae. Throughout the spine, all the vertebrae are designed the same except that the size and the mass increase from Cervical to Lumbar regions (Figure 3).

### Intervertebral Disc

Considering the entire height of the spine, the net disc height comprises of 20 - 33 %. The intervertebral disc consists of three main parts (Figure 3).

Nucleus Pulposus. This is located at the center of the disc, and is composed of a very loose and translucent network of fine fibrous strands that lie in a mucoprotein gel containing various mucopolysaccharides. The water content ranges from 70 - 90 % and tends to decrease with age. The lumbar nucleus fills 30 - 50 % of the disc cross sectional area. In the low back, the nucleus is usually more posterior than central and lies at about the juncture of the middle and posterior thirds of the sagittal diameter. The size of the nucleus is greater in the lumbar region.





Two Views of a Typical Lumbar Vertebra

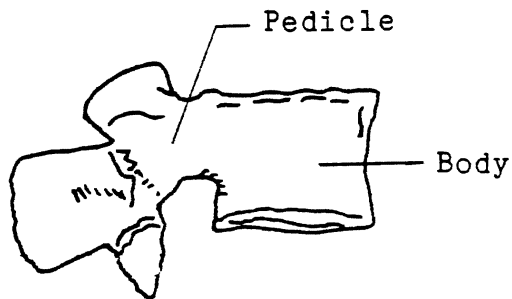


Figure 3. Anatomy of the Disc and the Vertebra

Annulus Fibrosis. This forms the outer boundary of the disc which is gradually differentiated from the boundary of the nucleus. This structure is composed of fibrous tissue in concentric laminated bands. These fibers are arranged in a helical structure. They run in about the same direction in a given band but in opposite directions in any two adjacent bands. They are oriented at 30 deg. to the disc plane.

Cartilaginous End Plate. The annulus fibers are attached to the cartilaginous end-plates in the inner zone. It is composed of hyaline cartilage that separates the other two components of the disc from the vertebral body.

The intervertebral disc has many functions and is subjected to a variety of forces and moments. In fact it is responsible for carrying all the compressive loads imposed on the trunk. The forces acting on a disc when a person is standing are much greater than the actual weight of the portion of the body above it. The force on a lumbar disc in a sitting position is determined to be more than three times the weight of the trunk. When dynamic load imposing activities like jumping and trauma are involved, the loads on the disc are much higher - as high as twice of those in static positions. These mainly result in compressive stresses. Tensile stresses are produced in certain portions of the disc during physiological motions of flexion, extension and lateral bending. Axial rotation of the torso

with respect to the pelvis causes torsional loads resulting in shear stresses in the disc.

The loads imposed on an intervertebral disc can be divided into two main categories according to the time duration of application:

- a. Short duration high amplitude loads.
- b. Long duration low amplitude loads.

The disc has certain time dependant properties such as fatigue and viscoelasticity characterized by hysteresis, creep and relaxation. Short duration loads cause irreparable structural damage to the disc when a stress higher than the ultimate failure stress is generated at a certain point in the disc. The mechanism of failure during long duration loading of relatively low magnitude is entirely different and is due to fatigue failure.

### Hysteresis

When an element is subjected to repetitive load and unload cycles, there is loss of energy. This phenomenon is called hysteresis. When a person jumps up or down, the shock energy is absorbed in between the feet and the head by the discs and veterbrae due to hysteresis. Hysteresis seem to vary with the load applied and the age of the disc, as well as its level. The larger the load, the greater the hysteresis. It is maximum in young people and minimum in the middle aged. It was observed that hysteresis decreased when the disc was loaded the second time. From this we may infer

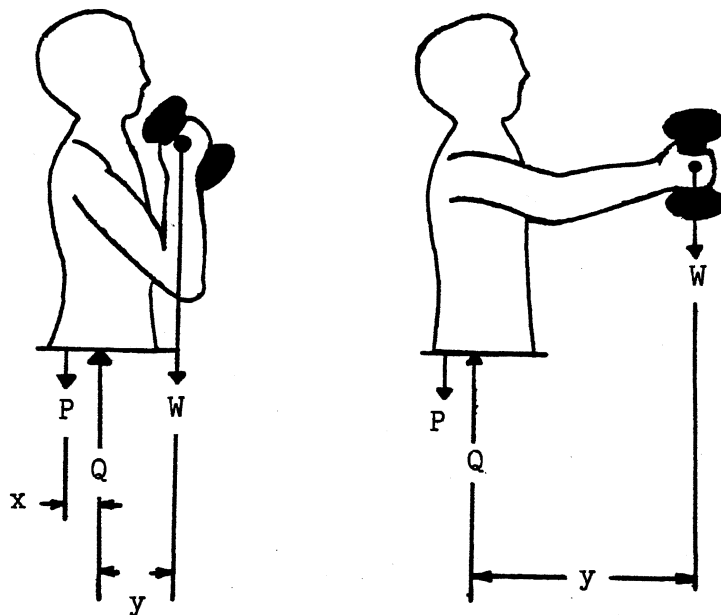
that we are less protected against repetitive loads. Epidemiologic studies show that people who drive motor vehicles have a higher incidence of herniated discs. The repetitive axial vibrations may be the prime factor.

#### Loads Imposed on Spinal Column

The difficulty lies in estimating a certain combination of the loads that represent the reality, because the exact loads in-vivo are not fully known. It was observed that the lamina is highly strained when the spine is inclined anteriorly and less so when inclined posteriorly. The motion segment provides greater resistance to failure when the loads are applied centrally rather than eccentrically or at some inclination. These observations would suggest that in lifting a weight, the spine should be kept as much in vertical position as possible.

#### Bending

The vertebral arch has a cross section that is especially suitable for taking up bending loads. The moment of inertia of an elliptical cross section is greatest for the bending loads in the direction parallel to its major axis. Fibers on the concave side of the bent structure are compressed, while those on the convex side are elongated. It was observed, in-vivo, that the disc pressure and the axial load in the lumbar region increase when a person while



Assuming the external weight  $W$  is balanced by only two internal forces :

$$Q = W + P$$

$$Q = W (1+y/x)$$

$$P \cdot x = W \cdot y$$

Figure 4. Estimation of Lumbar Trunk Loads

sitting reaches and picks up a book which is at distance. The reason for this increase is that the weight of the book results in a substantial bending moment at the disc due to the long lever arm. This bending moment is counterbalanced by the bending moment provided by muscle and ligamentous forces, which have a much smaller lever arm and hence must exert large forces in order to maintain equilibrium (Figure 4).

### Torsion

Since the lumbar spine is a curved structure, it is subjected to combined torsion and bending loads by simple axial rotation of the trunk with respect to the pelvis. Disc failure in low back pain may be due to these loads.

### Fatigue, its Effects and Importance

Fatigue tests on the disc are important for establishing the number of load cycles which can be tolerated before failure occurs. As the biological capacity for repair and regeneration of the disc are thought to be low, its fatigue properties are important.

The lumbar region, which is located at the base of the spine is a critical zone because it bears high loads. The lumbar zone has been the topic of intensive research by many investigators.

Adams and Hutton [9] performed tests on the lumbar intervertebral joints. 18 specimens were flexed and loaded at a rate of 40 cycles/min for 4 hours, to simulate a vigorous day's activity. 23 out of 41 discs showed distortions in the lamellae of the annulus fibrosus and in a few of these, complete radial fissures were found in the posterior annulus. The appearance of fissures suggest a slow distortion of the lamellae in response to chronic loading or fatigue rather than sudden injury. Liu et al., [10] carried out low-cycle fatigue tests on 11 lumbar intervertebral joints applying cyclic compressive loads on an MTS machine at a rate of 30 cycles/min for 5.5 hours. The results have been represented as displacement vs cycles/time. It was observed that after 6000 cycles, the rate of maximum displacement increased as a function of the number of applied cycles i.e., the slope of the curve is constant. This slope was noted to increase with an increase in the loading level for a given segment level. Hardy et al., [14] conducted repeated transverse bending tests on 9 specimens with a frequency of loading of 120 cycles/min for 18 hours. Nucleus pulposus was observed to be ruptured and the discs were noticed to be pushed anteriorly. Liu et al., [7] conducted torsional fatigue tests on 24 lumbar intervertebral joints using an MTS machine. An axial compressive preload of 440 N to simulate the supraincumbent torso weight was also applied and was held constant throughout the experiment. A frequency of 30 cycles/min was used.

Failures observed were facet cracks, torn capsules, tears in annulus and lamina cracks. Important contributions were also made in the field of three dimensional kinematics. Soni et al.,[1-5] have presented the three dimensional kinematics of the lumbar spine. In their investigations, they were able to identify variations in the kinematic properties with respect to age, sex and disc levels.

All these studies are limited to conducting isolated fatigue experiments on human spine and experiments investigating the kinematics of the lumbar spine. However there is a need to investigate the effect of cyclic loading on the mobility of the human spine. Of particular importance is to study the three dimensional kinematics of the normal human spine and the spine subjected to fatigue loading.



## CHAPTER II

### PROPOSED RESEARCH

#### Objectives

The objective of this research is to study the effects of a variety of loads on different human lumbar intervertebral joints and to observe the mobility of motion segments. This study will be achieved by subjecting the lumbar vertebral specimens to different types of loads with the help of specially designed fixtures. The following events are to be carried out in meeting the objectives of the proposed research.

- a. To design and fabricate the necessary fixtures to apply the required cyclic loads.
- b. To conduct different fatigue tests on the Lumbar Intervertebral Joints.
- c. To test the mobility of the motion segments at various cycles of load application.
- d. To monitor the experiments with the aid of an IBM AT Micro Computer through a DT2805 A/D - D/A converter.

## CHAPTER III

### THE FATIGUE TESTING APPARATUS

The objective of this research study is to conduct different fatigue loading tests on the lumbar intervertebral joints and observe the resulting effect of the laxity of the specimen. In order to subject the joints to a variety of loads including combined loads, special fixtures had to be designed and built.

The fatigue testing apparatus mainly consists of the following parts.

- a. Loading applying mechanism
- b. Fixtures to hold the vertebrae
- c. Compressive preload arrangement
- d. Cyclic load attachment
- e. Load measuring setup

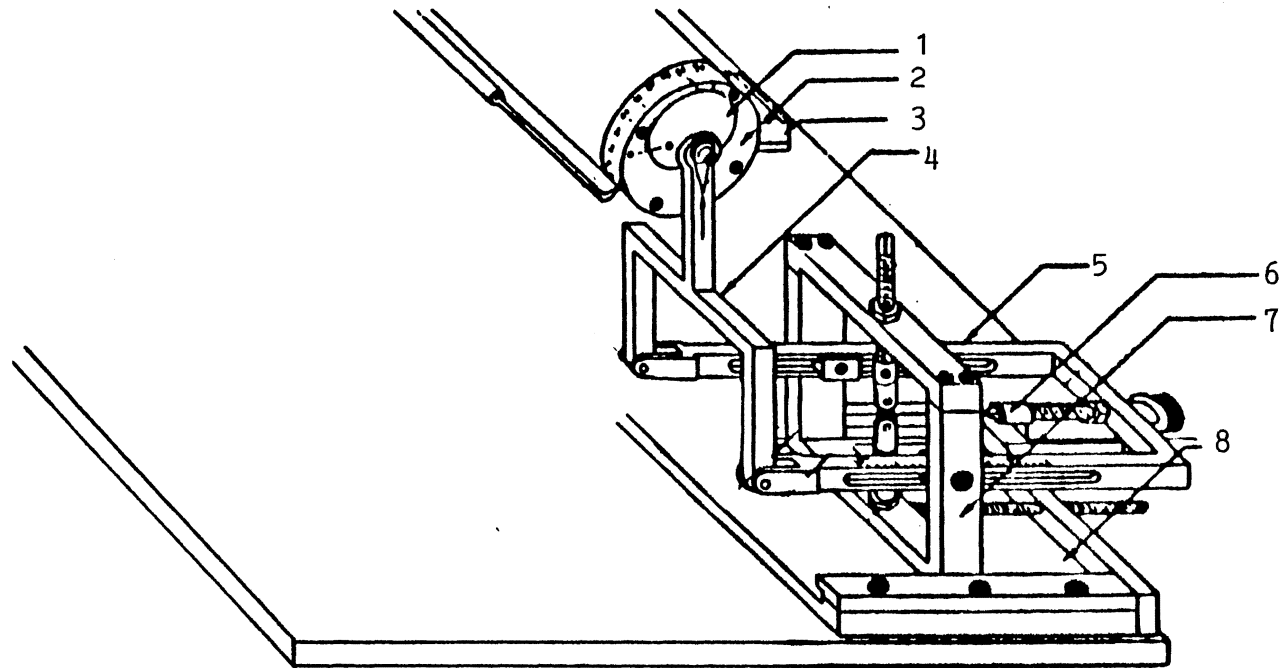
#### Loading Applying Mechanism

This is a compact bench mounted unit consisting of a rigid frame, variable throw crank, cyclic counter and variable speed drive (Figure 5). The mechanism is driven by a 1.5 HP, 115 Volts variable speed motor which is directly mounted on the bed through a pulley and belt arrangement. The speed is adjusted by a statotrol jr controller which is

connected to the motor. Force to the main shaft is derived from the motor and is transmitted through a four-link mechanism. The variable throw crank at the end of the main drive shaft acts as the driving link of the mechanism and transmits the force through a rigid coupler link to the output link. The output link, which is extended beyond the pivot joint, oscillates about the pivot joint which is a revolute pair. This oscillating motion of the output link is the source for applying bending and torsional loads to the intervertebral specimens. The effective length of the output link which is the length between the coupler link joint and the pivot joint can be varied by sliding the coupler link about the pivot joint along the longitudinal slots provided in both arms of the output link.

The input is given by the variable throw crank. The stroke has a range of 0 to 1.5 inches and is adjusted by loosening the four socket head screws around the face of the crank and adjusting the socket head screw about the eccentric. The coupler link, also called the connecting rod rides on a precision bearing.

A flywheel is mounted on the main drive shaft. The transmitted force as absorbed by the specimen and the loading fixture is never uniform during the cycle. The flywheel serves as a means to store energy during the period of time when not much energy is needed to drive the output link and to release the energy in that period when some extra energy is needed to drive the output link.



1. Variable throw crank      2. Crankhead assembly  
3. Cycle counter      4. Coupler link      5. Output link  
6. Attachment      7. Supporting frame      8. Adjustable vise

Figure 5. Load Applying Mechanism

The cycle counter is a six-digit unit which counts every 3 cycles. It is driven by a flexible shaft mounted inside an outer tubing.

#### Fixtures to Hold the Vertebrae

Special cups were built to hold the intervertebral specimens. 8 holes were drilled and tapped on the circumference of the cup at 45 degree angle separation on two planes, 4 on each plane. 4 of the holes take pointed rods which drill into the body of the specimen to secure it in place. The other four holes take 4 more rods which are used in testing the mobility of the motion segment. The cup is attached to a long rod to facilitate the application of required loads.

#### Compressive Preload Arrangement

A pneumatic cylinder attached to a compressed carbondioxide bottle is used in applying the compressive preload to the specimen. The rod from the cup slides in two bronze bushings mounted in a cylinder. A key arrangement between the cup rod and the bushings prevents the rod from any rotary motion. This rod is attached to the pneumatic cylinder piston rod through a self aligning coupler which compensates for any misalignment between the piston rod and the cup rod. The whole setup is mounted on a railing which is bolted to the bed of load applying mechanism. When the

pneumatic cylinder is activated by the compressed carbondioxide bottle it applies a constant compressive preload, to the specimen mounted in the cups, throughout the entire experiment. The regulator regulates the gas pressure and hence the load applied to the vertebral specimen is controlled.

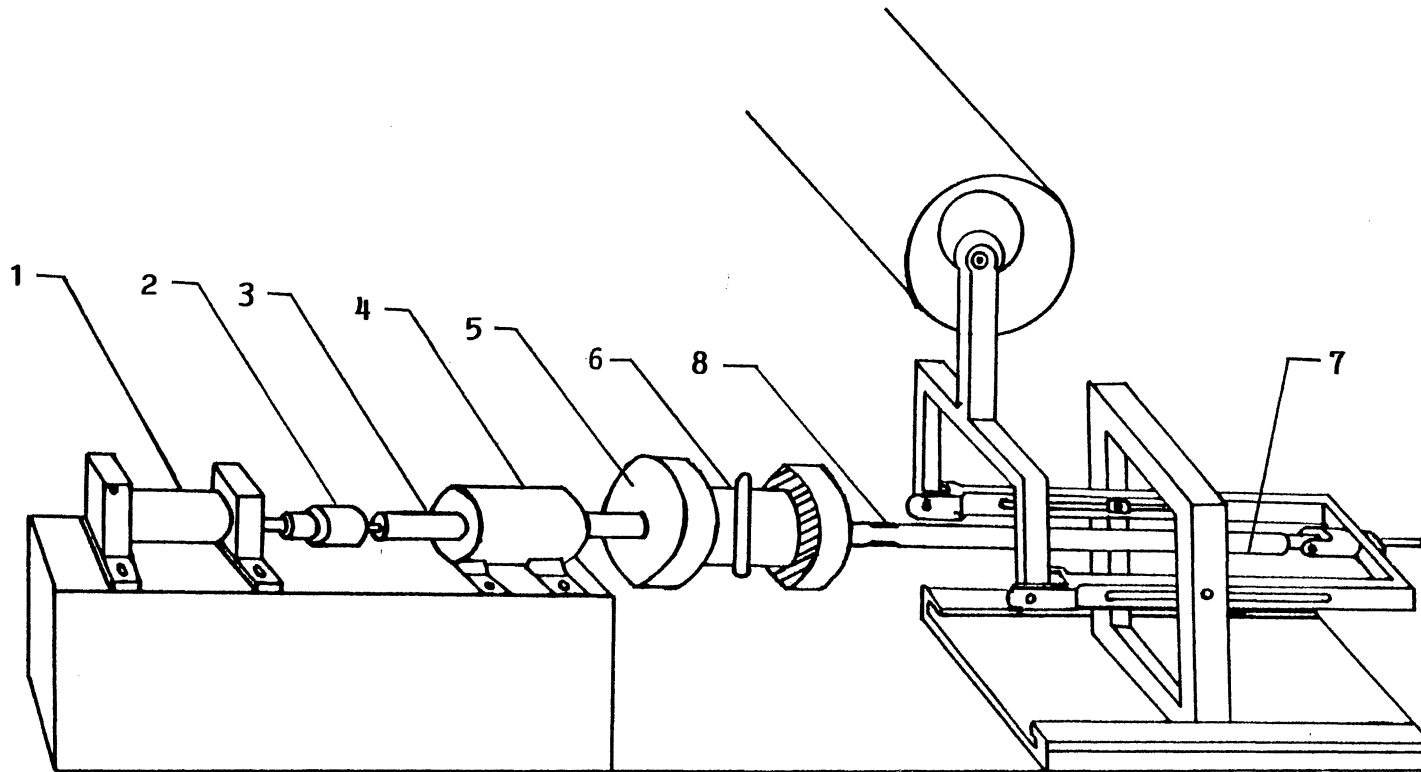
### Cyclic Load Attachment

#### Bending

The rod fixed to the base of the second cup is attached to the output link of the loading mechanism through a revolute pair to facilitate the application of bending load to the specimen. The rotary motion of the eccentric crank is translated as oscillatory motion to the output link. This motion of the output link applies bending load to the specimen. Strain gages are mounted on the cup rod to monitor the bending load (Figure 6).

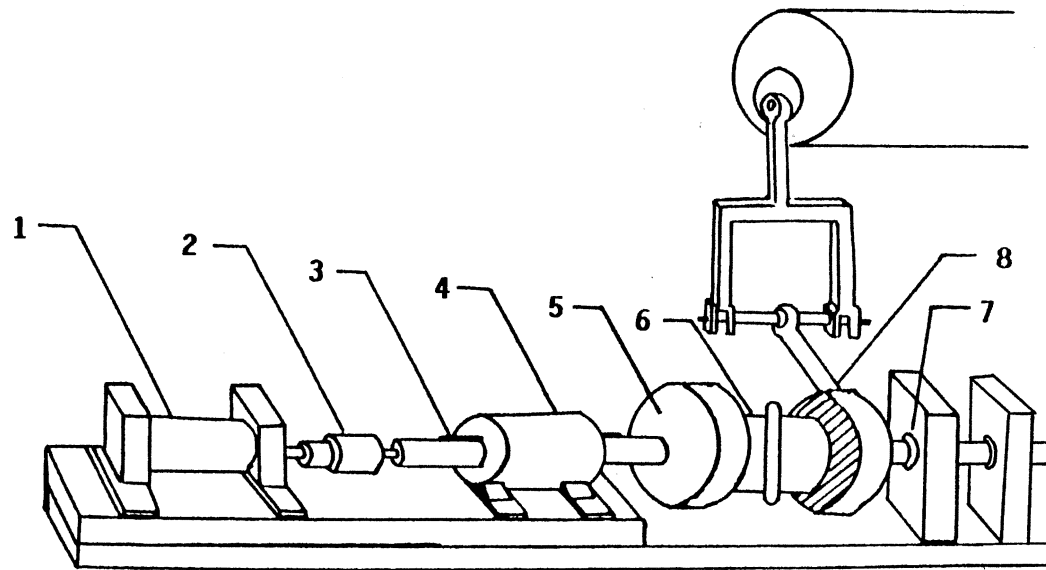
#### Torsion

A rod, which is fixed to the base of the second cup by a flange arrangement, is mounted in two self aligning pillar block bearings. The connecting link of the loading mechanism is attached to the cup rod through another small rod on which strain gages are mounted to monitor the torsional load. As the connecting link moves up and down, it rotates the cup rod and hence the cup (Figure 7).



1.Pneumatic cylinder 2.Coupler 3.Axial Rod 4.Bushing  
5.Cup 6.Specimen 7.Cup rod 8. Strain gages

Figure 6. Fixtures for Bending Fatigue Test



- |                       |                   |              |
|-----------------------|-------------------|--------------|
| 1. Pneumatic Cylinder | 2. Coupler        | 3. Axial rod |
| 4. Bushing            | 5. Cup            | 6. Specimen  |
| 7. Bearing            | 8. Connecting rod |              |

Figure 7. Fixtures for Torsional Fatigue Test



### Load Measuring Setup

The bending moment or the torsional load applied to the vertebral joint is measured with the aid of two active strain gages mounted on either side of the load applying rod. The gages record equal and opposite strains as one monitors compression and the other tension. The gages are linked to the Vishay Strain Gage Amplifier which provides the circuit for the Wheatstone half bridge.

Strain gages are able to sense and respond to deformation. The measured quantity obtained from a strain gage is proportional to an average strain in the gage length of the gage. The basic principle involved is that a wire changes its electrical resistance when deformed. The resistance change which is accurately proportional to the strain is measured by the Vishay amplifier. Each gage has a gage factor which is a measure of the sensitivity of the gage. The gage factor is defined as the ratio of the unit change in resistance to the unit change in length.

$$GF = (\delta R/R) / (\delta L/L)$$

GF - gage factor

$\delta R$  - total change in resistance

$\delta L$  - total change in length

The gages presently used have a GF of 2.11.

The basic part of the load measuring setup is shown in Figure 8.

From Wheatstone bridge circuit, the relationship for a balanced bridge with zero output is :

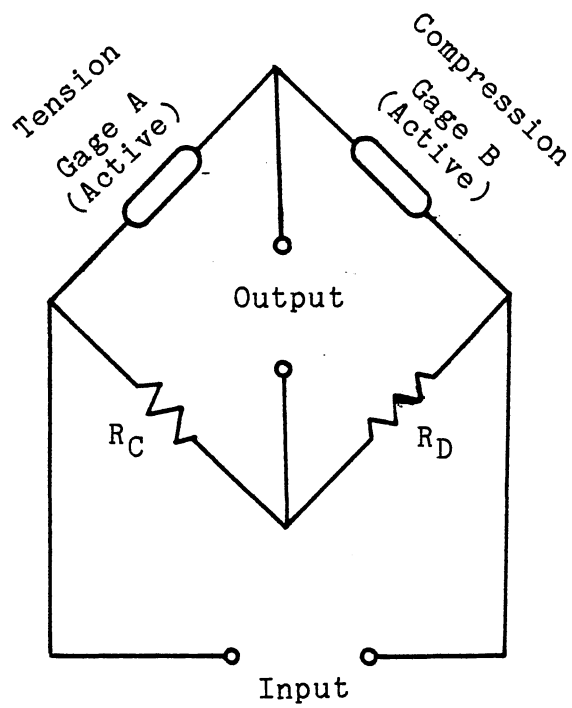
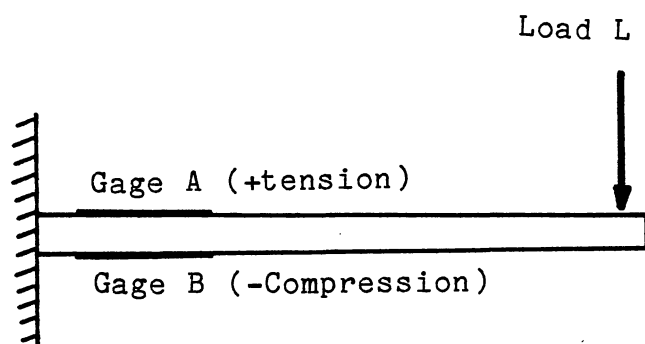


Figure 8. Basic Load Measuring Setup

$$R_A * R_D = R_B * R_C$$

When the rod is subjected to load L acting downward, gage A experiences tension and gage B experiences compression, thus causing the above equation to become unbalanced. The magnitude of this unbalance is measured as the output of the bridge and is proportional to the strain of the member. If tension in gage A in one arm of the bridge caused a certain unbalance resistance ( $+\delta R_A$ ) and , the compression in gage B caused an opposite change ( $-\delta R_B$ ), then the output is doubled. The equation for the circuit would then be

$$(R_A + \delta R_A) * R_D = (R_B - \delta R_B) * R_C$$

The output from the Vishay Amplifier is fed to the IBM AT personal computer through a DT2805 A/D - D/A converter. PCLAB routines are called to measure the dynamic voltage outputs. While measuring the dynamic loads a sampling interval of 0.025 sec is used. Thus for a dynamic load of frequency 30 cycles/min , 80 samples are taken per cycle. This sampling period is given to the PCLAB routine SET\_CLOCK\_DIVIDER in terms of number of 'ticks', each 'tick' being assigned a span of 2.5 microseconds. Thus 10,000 'ticks' are chosen for a sampling period of 0.025 sec.

Routine ADC\_SERIES is called to read the dynamic output voltage from the Vishay amplifier, where the sampling period of the output measurement is set by the routine SET\_CLOCK\_DIVIDER. Routine ADC\_VALUE is called to read the voltage outputs from the six potentiometers of the linkage

transducer which is used in the mobility test. A pascal program is written to call the required routines, which stores the data in different output files (see Appendix A).

#### Calibration of the Gages

Practically, the strain gages are calibrated by applying known loads and measuring the strain. The strain is converted into voltage through the Vishay Strian gage Amplifier. This voltage is recorded by the IBM AT personal computer through the 2805 A/D board. Calibration charts are shown as Load vs Voltage (Figure 9, Figure 10), for both bending and torsional load measurement.

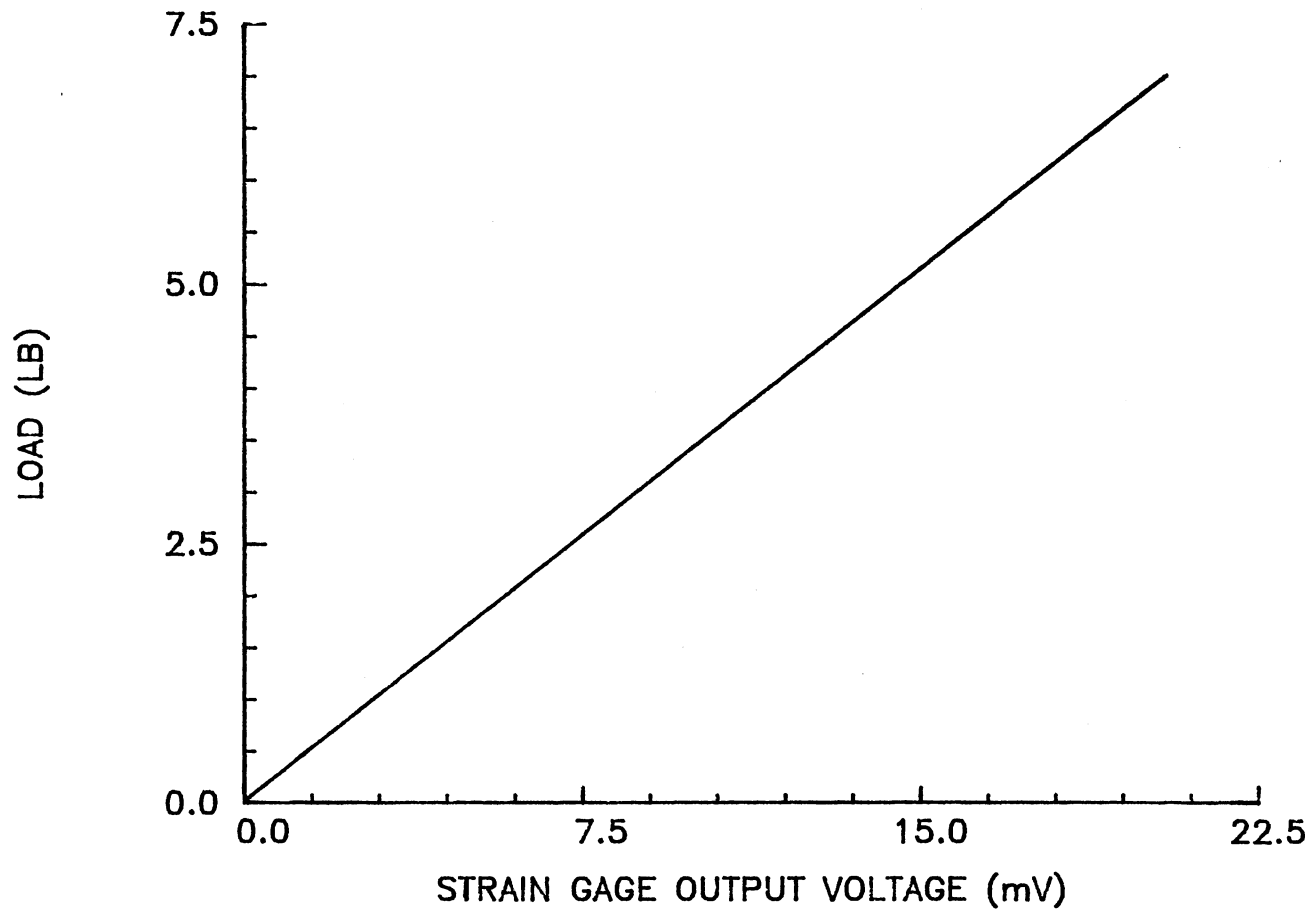


Figure 9. Calibration Curve for Bending Load Measurement

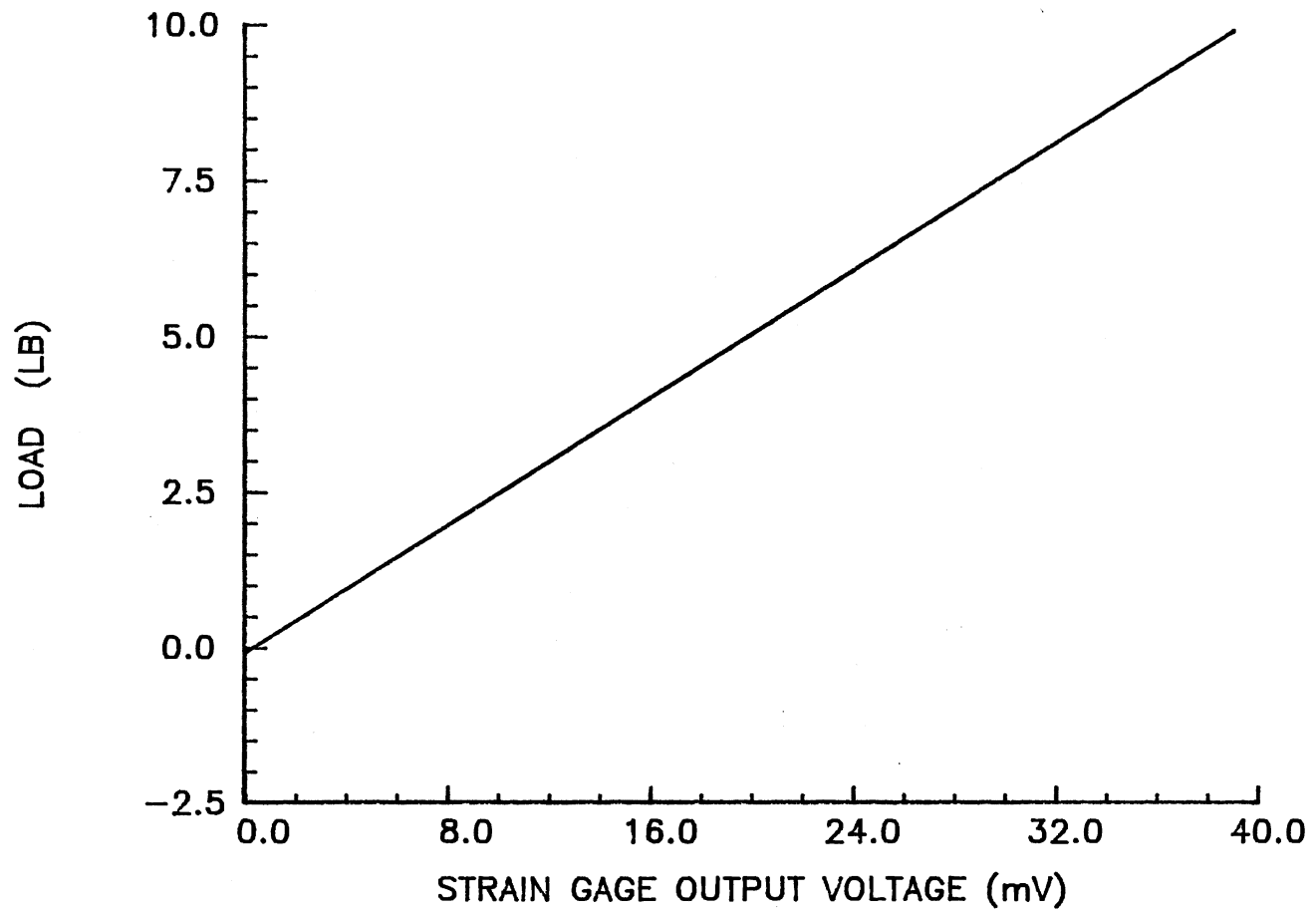


Figure 10. Calibration Curve for Torsional Load Measurement

## CHAPTER IV

### KINEMATICS OF SPINE

Kinematics is that science of mechanics which deals with the study of relative motion between rigid bodies. The manner in which a rigid body executes this relative motion defines the kinematic constraints. The vertebrae of the spine can be considered to behave as rigid bodies. An overall clear knowledge of spinal kinematics plays a supreme role in understanding the aspects of clinical analysis and management of spinal problems like spine trauma, scoliosis, low back pain etc.

#### Degrees of Freedom

A rigid body has six degrees of freedom if it moves freely in the three dimensional space without any constraints. That is, its motion can be basically condensed into six characteristic movements: three rotations and three translations about and along a set of three orthogonal axes. These six movements are called six degrees of freedom of the rigid body. The number of independent coordinates in a coordinate system required to completely specify the position of a rigid body in space are called the degrees of freedom.

The vertebra has all six degrees of freedom as the trunk is manipulated with respect to the pelvis.

### Representation of 3-D Displacement

In three dimensional motion, when a rigid body is displaced from one position to another position in space, its motion can always be described as a rotation about a certain axis and a translation along the same axis. This constitutes helical motion. This motion is analogous to the motion of a screw and the axis of the screw is the helical axis of motion. Thus the helical axis is also called the screw axis.

Totally there are six parameters associated with this representation (Figure 11).

1. Rotation  $\phi$  about the helical axis
2. Translation  $T$  along the helical axis
3. Two of the three direction cosines  $U_x$ ,  $U_y$ , and  $U_z$  describing the orientation of the helical axis with respect to the XOYZ reference frame.
4. Two coordinates  $P_x$  and  $P_y$  of the point of intersection of the helical axis with the XY reference plane.

Rotation  $\phi$  and translation  $T$  are known as the laxity parameters.

The screw axis representation is one of the most precise ways to define the three dimensional motion of a rigid body. The advantage in using this representatin to



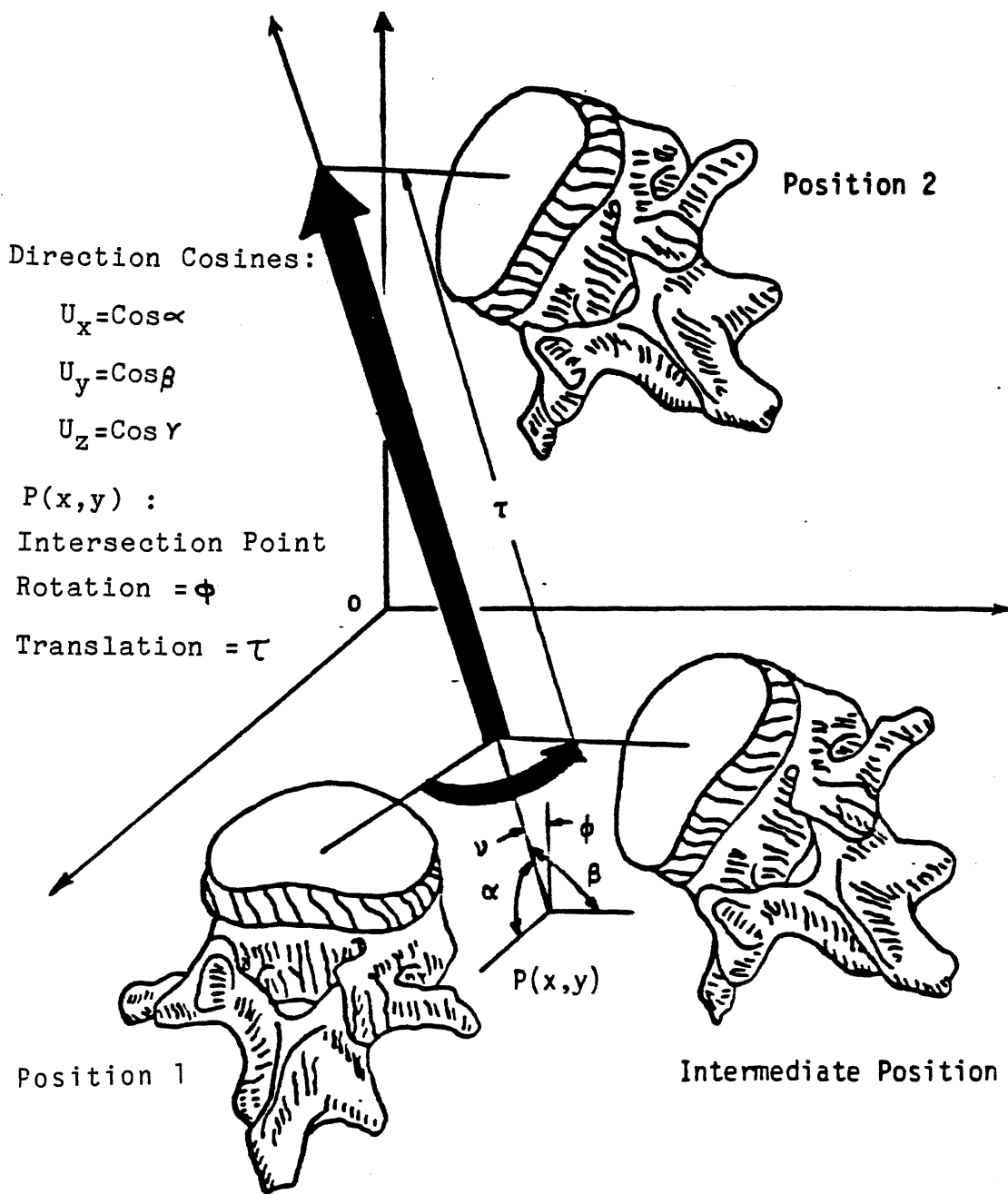


Figure 11. Screw Axis Representation

describe a three dimensional motion is that the Rotation  $\phi$  and the Translation T about and along the screw axis remain constant irrespective of the choice of the coordinate system.

### Motion Segment

The unit of study in spinal kinematics is called a Motion Segment or a Functional Spinal Unit. It represents the inherent biomechanical characteristics of the entire ligamentous spine. It consists of two adjacent vertebrae and their intervening soft tissues. The spine may be viewed as a structure composed of a number of motion segments connected in series and its total behaviour is a composite of the individual motion segments.

### Physiological Patterns of Motion

The traditional patterns of motion are classified as :

- a. Flexion/Extension
- b. Left/Right Lateral Bending
- c. Axial Rotation

Bending forward in the sagittal plane is flexion and bending backwards is extension. Spine is more flexible in flexion than in extension. Bending sideways in the frontal plane is left/right lateral bending (Figure 12).

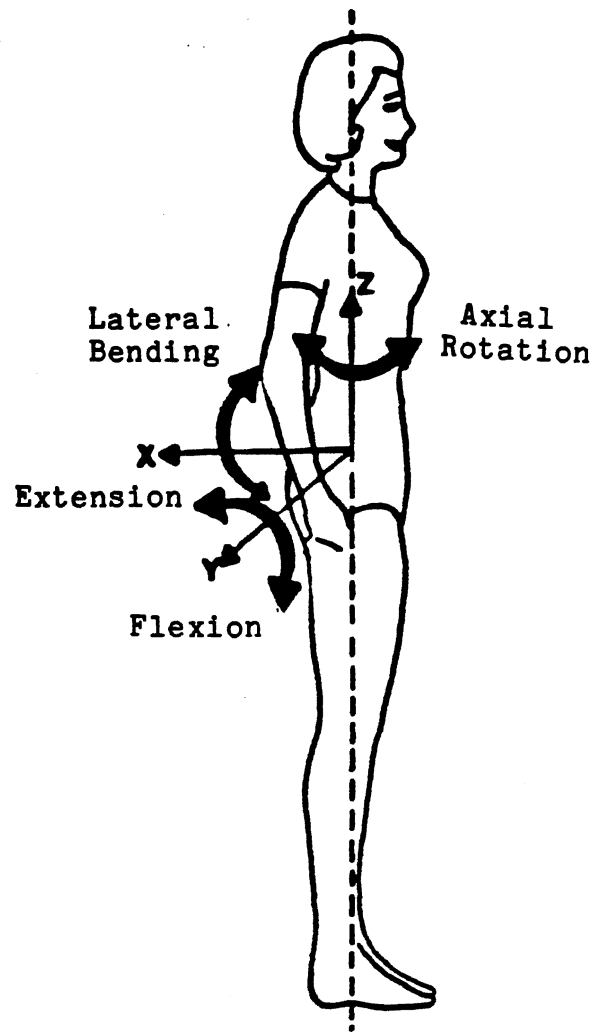


Figure 12. Physiological Patterns of Motion

## CHAPTER V

### MATERIALS AND METHOD

#### Specimen Preparation

Fresh spine specimens are obtained and the intervertebral joints, in the lumbar region, consisting of two vertebrae including the disc inbetween are processed. The motion segments are cleaned by stripping away all the fat and muscle, but leaving the ligaments intact. These specimens are stored in sealed plastic bags at  $-25^{\circ}$  C. The fact that storing spinal specimens at  $-25^{\circ}$  C does not alter the properties of the material is established by many investigators.

The frozen motion segments are thawed for 12 hours at room temperature before the actual testing. Each motion segment is comprised of two adjacent vertebrae with its intervening disc and ligamentous soft tissues.

#### Specimen Mounting

Each vertebra of the motion segment is mounted in a cup specially designed to secure the specimen. First, a layer of Plumbers Putty is laid at the bottom of the cup. The thickness of this layer is dependent on the size of the

specimen. By varying the thickness of the plumbers putty in the cup, the height of the vertebra relative to the cup is varied.

The specimen is mounted inside the cup (fixed cup) making sure that :

- a. the center of the vertebral specimen coincides approximately with the center of the cup.
- b. the plane of the intervertebral disc is parallel to the base of the cup.
- c. about half of the vertebra is outside the cup.

Four steinman pins going through four holes on the circumference of the cup, which are at 90 degree separation to each other, are drilled into the cellulous bone of the vertebra.

Bone cement is then poured in the cup, to the brim, covering the four rods securing the vertebra. Bone cement is a dough-type, radiopaque material comprising of a mixture of methyl methacrylate monomer and poly (methyl methacrylate) containing barium sulphate as opacifier. Bone cement, which solidifies in about 30 minutes, is a high strength material which excellently secures the vertebra, making it integral with the cup.

The second vertebra of the motion segment is mounted in another cup (moving cup) following the same procedure ensuring that the bases of the two cups are parallel to each other with the help of a spirit level.

When applying bending or torsional loads, one cup is

fixed while the other cup is moved and hence the notation fixed cup and moving cup.

### Mobility Test

The data for the mobility test is collected at various cycles of the fatigue loading with the aid of linkage transducer. The linkage transducer is made up of seven links, and six rotary potentiometers. The transducer has negligible weight and does not load the specimen. It also does not interfere with the actual intervertebral motion to be measured. The data collection procedure is controlled by means of an IBM AT personal computer, with user interaction through a DT 2805 A/D - D/A converter. The six potentiometers of the transducer are connected to the six channels of the A/D - D/A converter. Pascal program is written to call the PCLAB routines to measure the static voltage output from the six potentiometers (see Appendix A).

The motion segment along with the cups is detached from the loading mechanism and is transferred to a special fixture designed to conduct the mobility test (Figure 13). This fixture consists of a base to which the fixed cup is tightly secured. The spine motion segment is able to execute its normal mode of motion in the frontal plane, sagittal plane and any other plane in between. The mobility fixture consists of a rotating circular base carrying four vertical bars and a horizontal bar. Shear and moment loads can be applied to the motion segment by means of cables, pulleys

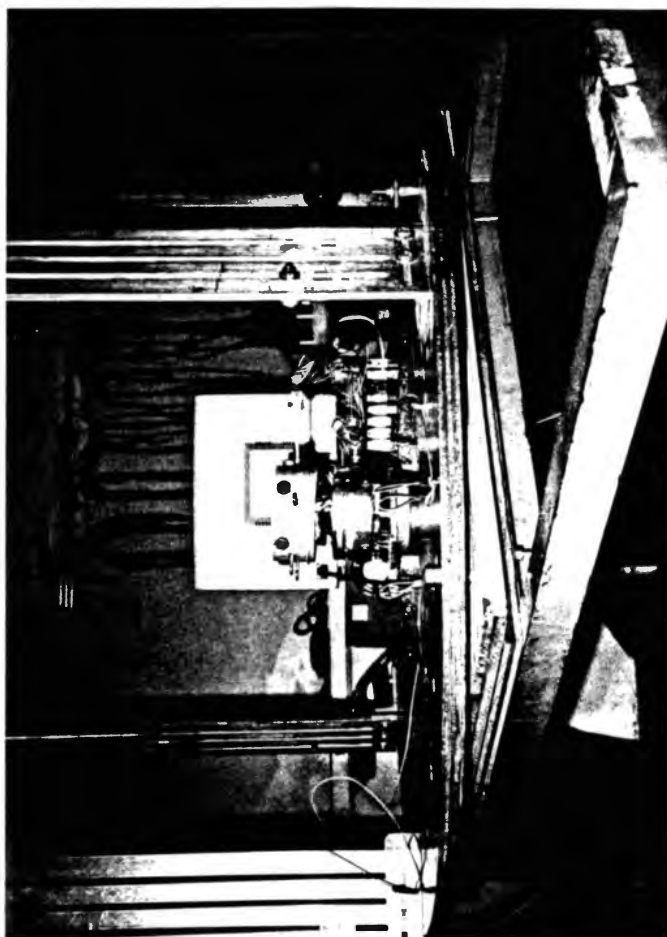


Figure 13. Fixture for Mobility Test

and static weights. One end of the cable is attached to the top cup and the other end to a loading pan through a system of pulleys attached to the horizontal and vertical bars. The first link of the linkage transducer is attached to the fixed cup in a plane coincident with the sagittal plane of the vertebrae. The last link of the transducer is attached to the moving cup in a plane inclined at 45 degrees to the sagittal plane.

Different types of loads are applied to the moving cup both in the sagittal plane (0 degrees) and the frontal plane (90 degrees). For each type of load, the output from the six potentiometers of the linkage transducer are recorded by the computer as AD values.

The forces and moments which are applied while testing the mobility of the motion segment can be identified in engineering as well as in anatomical terms. These are summarized in Table 1 with reference to Figure 14.

The AD values obtained from the computer are transferred to the program developed on the IBM 3081K mainframe, where they are processed to give the six degrees of freedom of the motion segment for each load.



TABLE I  
SUMMARY OF LOADS APPLIED ON THE MOTION SEGMENT

Magnitude/ Direction	Plane of Application	Force/Moment
+ $F_x$	Sagittal	Posterior Shear (0° Positive Shear)
- $F_x$	Sagittal	Anterior Shear (0° Negative Shear)
+ $F_y$	Frontal	Right Lateral Shear (90° Positive Shear)
- $F_y$	Frontal	Left Lateral Shear (90° Negative Shear)
+ $M_x$	Frontal	Left Lateral Moment (90° Negative Moment)
- $M_x$	Frontal	Right Lateral Moment (90° Positive Moment)
+ $M_y$	Sagittal	Extension (0° Positive Moment)
- $M_y$	Sagittal	Flexion (0° Negative Moment)
+ $M_z$	Horizontal	Left Rotation (Positive Torque)
- $M_z$	Horizontal	Right Rotation (Negative Torque)

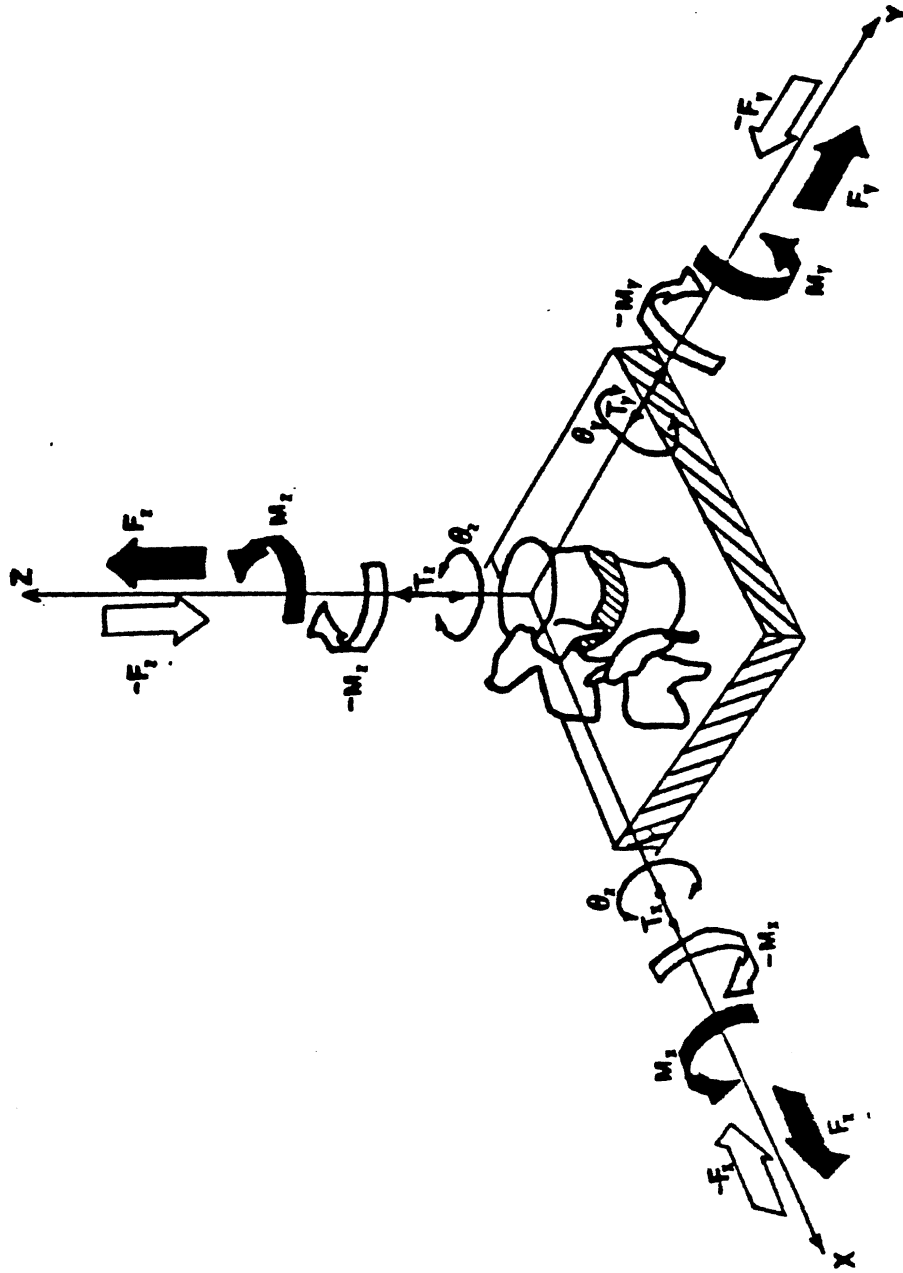


Figure 14. Loads Applied on the Motion Segment

## CHAPTER VI

### DATA ANALYSIS AND CONCLUSIONS

A total of three tests are conducted in order to observe the kinematics of lumbar motion segments under different fatigue loads. The six degrees of freedom of the motion segment are calculated at specified cycles of load application. The motion segment is subjected to different types of loads while conducting the mobility test - Positive Shear (PS), Negative Shear (NS), Positive Moment (PM), Negative Moment (NM), Positive Torque (PT) and Negative Torque (NT). These loads are applied both in the sagittal and the frontal planes. Thus the data analysis is done with respect to the sagittal and the frontal planes.

The variation of Rotations and Translations are represented as bar charts, the height of each bar representing the respective magnitude. The instantaneous points of intersection of the Screw Axis with the respective planes are also plotted in order to observe the trend.

## Experiment 1

This test is conducted to observe the variation of peak bending fatigue load with respect to the number of cycles, the angle of bending remaining constant.

Type of Loading : Bending in the Sagittal Plane with  
Compressive Preload

Motion Segment Level : L3-L4

Frequency of Bending : 36 cycles/min

Angle of Bending : 8 degrees

Magnitude of Compressive Preload : 106.2 LB

Total cycles of load application : 2250

The variation of bending moment with respect to the number of cycles of load application is shown in Figure 15.

### Results

After 2000 cycles of load application, it is observed that there is a drop of 19 percent in the bending moment.

This shows that the resistance to the external load

Bending With Compressive Preload

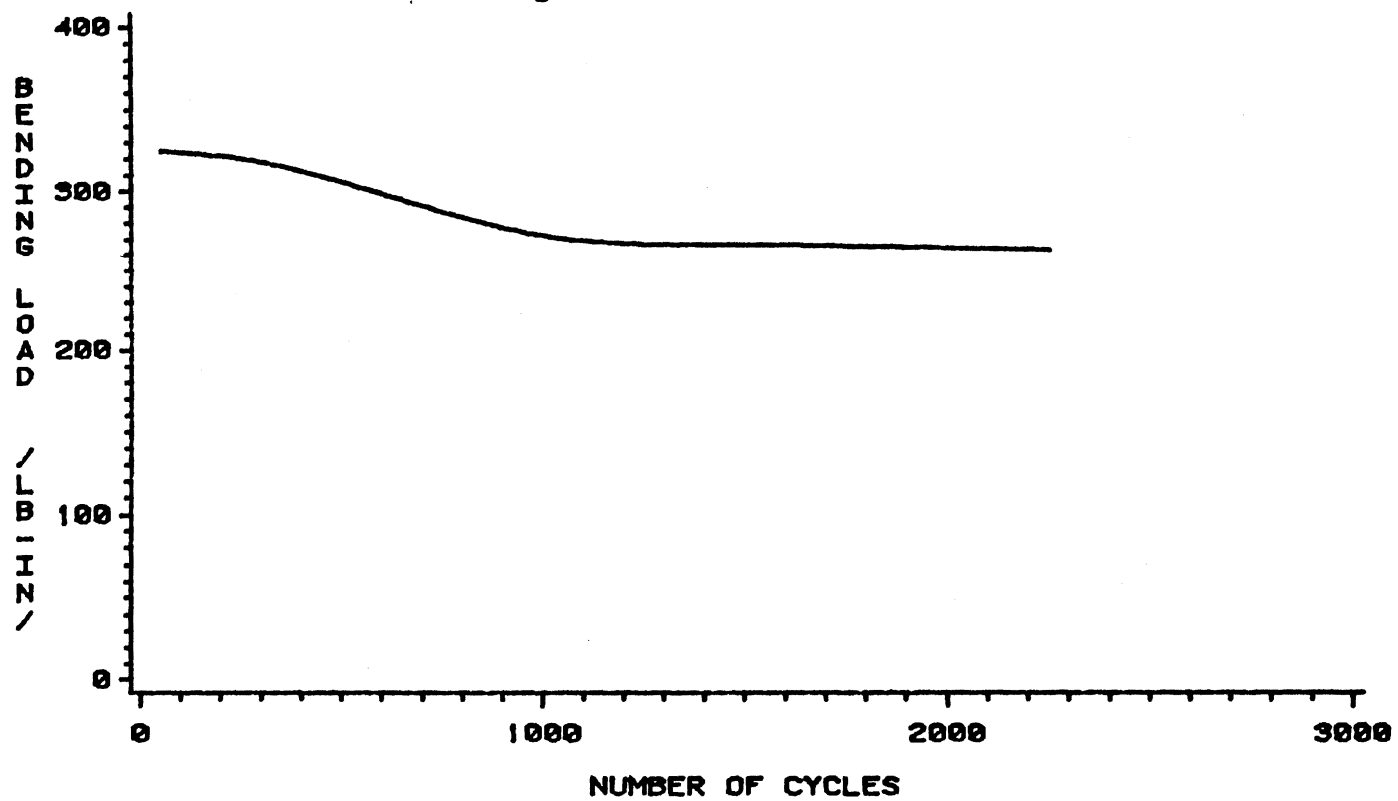


Figure 15. Variation of Bending Load

decreases with the increase in number of cycles, thus increasing the laxity of the specimen.

No visual damage is observed except that some fluid is noticed to ooze out of the joint while the load is being applied.

## Experiment 2

This test is conducted to observe the variations of the degrees of freedom of the motion segment subjected to cyclic torsional fatigue load. The mobility of the motion segment is tested at three different phases of the load application.

Type of Loading : Pure Torsion

Motion Segment Level : L1-L2

Frequency of Torsion : 30 cycles/min

Angle of Torsion : 2 degrees

Total cycles of load application : 5050

Initial peak torsional load (300 cycles) : 247.17 in-lb

Final peak torsional load (5050 cycles) : 223.96 in-lb

Net decrease in the torsional load : 9.4 %

Mobility tested at : a) 0 cycles  
b) 2020 cycles  
c) 5050 cycles

## Results

The variation of the laxity parameters, Rotation and Translation, are represented in Figure 16 through Figure 29, the height of each bar representing the magnitude. As the cycles of load application increased, it can be observed from Figure 16 and Figure 24, that the rotations about the Screw Axis increased in all type of loads.

The laxity parameter, rotation, has increased by 62 percent under the application of posterior shear, 34 percent under anterior shear, 4 percent under extension, 80 percent under flexion, 23 percent under right lateral shear, 29 percent under left lateral shear, 7 percent under right lateral bending, 27 percent under left lateral bending, 29 percent under left rotation and 46 percent under right rotation. Comparing all the shear loads, most significant increase is observed under the application of posterior shear (62 percent). Considering all the bending loads, flexion recorded the highest increase (80 percent). Extension and right lateral bending recorded low increase, 4 percent and 7 percent respectively. Under torsional loads, right rotation showed the highest increase (46 percent).

Considering the three rotations  $R_x$ ,  $R_y$  and  $R_z$  about the three orthogonal axes, the rotation  $R_y$  under posterior shear showed a constant increase. Under anterior shear,  $R_z$  showed a constant increase, 64 % being the net rise.

The variation of translations, which are shown in Figure 17 and Figure 25, did not follow a definite pattern,



except that under right rotation a gradual increase has been observed. Between 0 and 2020 cycles the increase recorded is 90 percent and between 2020 and 5050 cycles it is 43.3 percent. Thus the final result showed a total increase of 171 percent.

The points of intersection of the Screw Axis with the XY plane under torsional load are shown in Figure 30. The cycles of load application are marked at each point on the figure. The points for right rotation and the points for left rotation are observed to occupy two distinct regions on the XY plane.

Drop in the peak torsional load has been observed to be 9.4 percent.

## Experiment 3

This test is conducted to observe the variations of the degrees of freedom of the motion segment subjected to cyclic bending fatigue load. The mobility of the motion segment is tested at three different phases of the load application.

Type of Loading : Pure Bending

Motion Segment Level : L3-L4

Frequency of Bending : 30 cycles/min

Angle of Bending : 10 degrees

Total cycles of load application : 5280

Initial peak bending load (180 cycles) : 132.86 in-lb

Final peak bending load (5100 cycles) : 108.03 in-lb

Net decrease in the bending load : 18.7 %

Mobility tested at : a) 0 cycles

b) 2010 cycles

c) 5280 cycles

## Results

The variation of the laxity parameters, Rotation and Translation, are represented in Figure 31 through Figure 44 the height of each bar denoting the respective magnitude.

From Figure 31 and Figure 39 it is obvious that the rotations about the screw axis increased as the number of cycles of load application increased under all loads. The laxity parameter, rotation, has increased by 22 percent under the application of posterior shear, 56 percent under anterior shear, 41 percent under extension, 80 percent under flexion, 42 percent under right lateral shear, 16 percent under left lateral shear, 39 percent under right lateral bending, 21 percent under left lateral bending, 37 percent under left rotation and 81 percent under right rotation. Comparing all shear loads, most significant increase is observed under the application of anterior shear (56 percent). Significant increase in rotation is observed under flexion than in extension supporting the fact that the spine is more flexible under flexion. Also, considering all the bending loads, flexion recorded the highest increase (80 percent). Under torsional loads, right rotation showed higher increase (81 percent).

Rotation  $R_z$  showed a constant increase in magnitude under posterior shear. Flexion recorded a constant increase in magnitude in rotation  $R_y$ . Left lateral bending showed a consistent rise, 20.67 percent being the net.

Laxity parameter Translation did not particularly show a definite pattern in variation except that under flexion, a constant increase is observed and right rotation recorded a constant decrease. Figure 45 represents the points of intersection of the Screw Axis with the XY plane under the application of torsional loads. The cycles of load application are marked at each point on the figure. The points for right rotation and left rotation are observed to occupy distinct regions on the XY plane. The drop in the peak bending load has been observed to be 18.7 percent.

## Conclusions and Recommendations

The laxity parameter, rotation, under all loads showed a distinct increase as the cycles of load application increased.

These results clearly indicate that the increase in rotations with the increase in the cycles of load application gives us a measure of the flexibility of the motion segment. In both experiments, comparing all bending loads, highest increase in the laxity parameter rotation is recorded under flexion.

Role of the laxity parameter, translation, in understanding the laxity of the motion segment did not particularly point out to a definite trend, though, under some loads it is observed to increase.

The points of intersection of the Screw Axis with the XY plane under counter clockwise torque and clockwise torque are observed to occupy distinct regions in both the experiments. This does not throw much light on the movement of the screw axis as related to the kinematics of the motion segment and does not point out to a particular trend. The reason for selecting the XY plane for the points of intersection is that the torsional loads are applied about the Z axis and obviously the Screw Axis should intersect with a plane perpendicular to the Z axis, which is the XY plane.

There are drops in the torsional fatigue load and the bending fatigue load indicating that the resistance to

external load decreases with increase in the cycles of load application and thus increasing the laxity of the specimen. This drop has been observed to be more in bending(18.7 percent) than in torsion(9.4 percent).

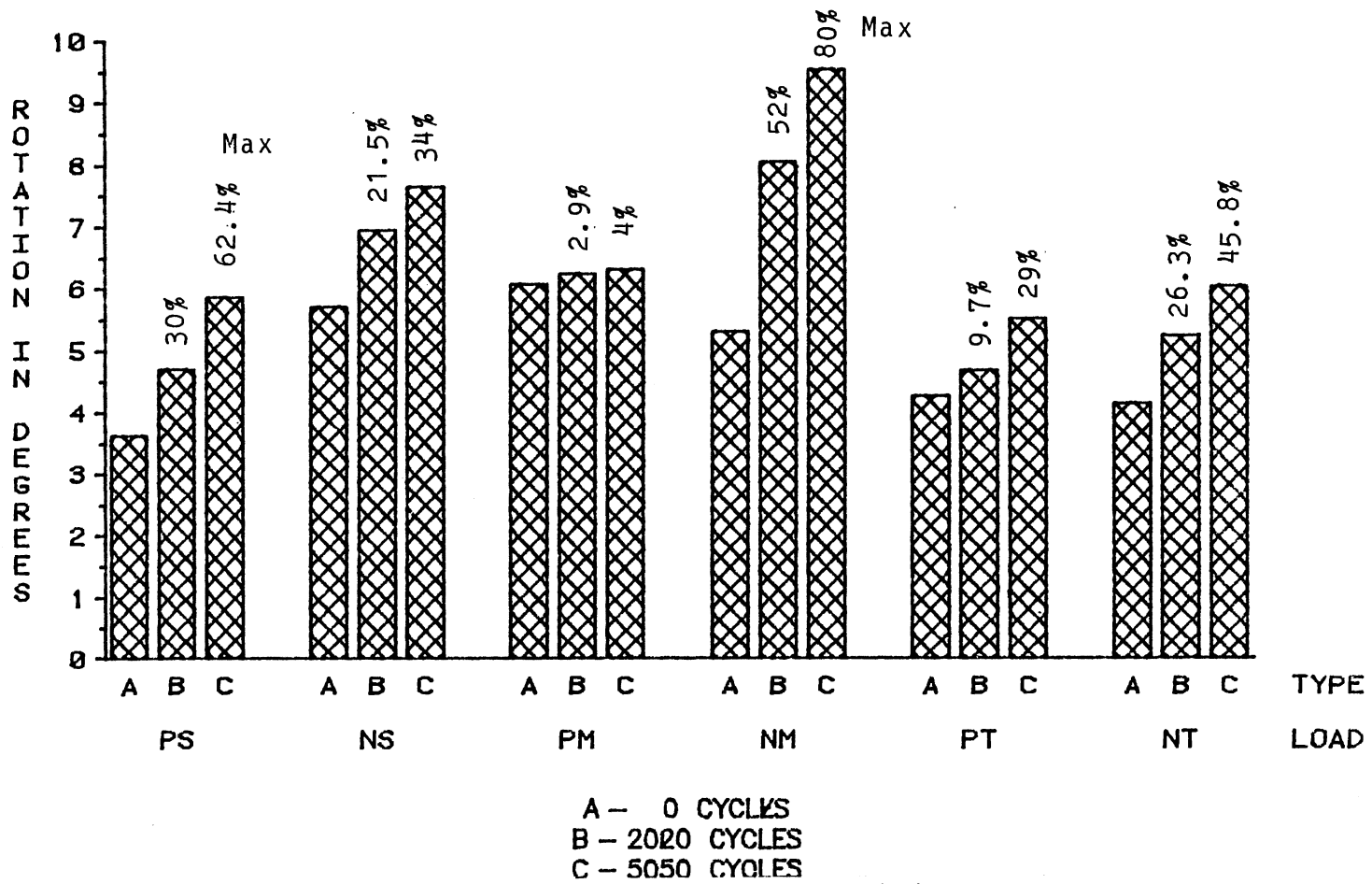
As the motion segment represents the inherent biomechanical characteristics of the entire spine, these results throw light on the three dimensional kinematics of the spine itself. The numerical data gives a clear relationship between the flexibility of the intervertebral joint and the cycles of load application in terms of the laxity parameters.

From the cadaver study, realizing the limitations of in-vivo situations, we may conclude that the laxity of the spine increases with increased physical activity involving enhanced movements of the spine.

#### Future Scope

This study significantly contributes to the understanding of the three dimensional kinematics of the human spine. However, the following possible extensions are suggested in view of expanding the scope of the study.

- a) To increase loading cycles upto 100,000
- b) To conduct mobility test at more than three phases of load application
- c) To apply constant peak fatigue load
- d) To apply compressive preload



A - 0 CYCLES  
 B - 2020 CYCLES  
 C - 5050 CYCLES  
 Percentage increase with respect to  
 0 cycles is indicated on the top of each bar

Figure 16. Rotations for Different Loads (0 deg.) Under Torsional Fatigue Load

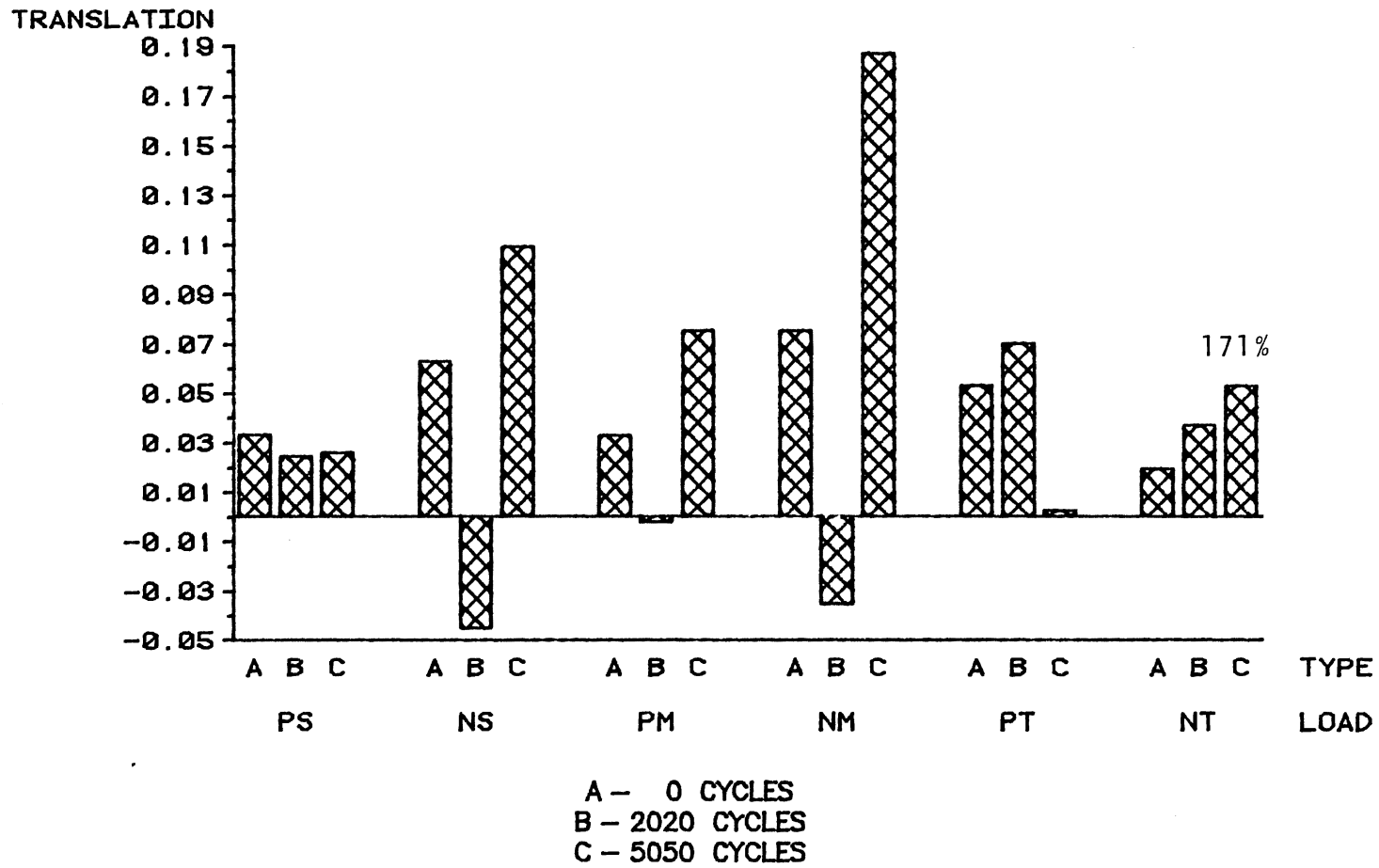


Figure 17. Translations for Different Loads (0 deg.) Under Torsional Fatigue Load



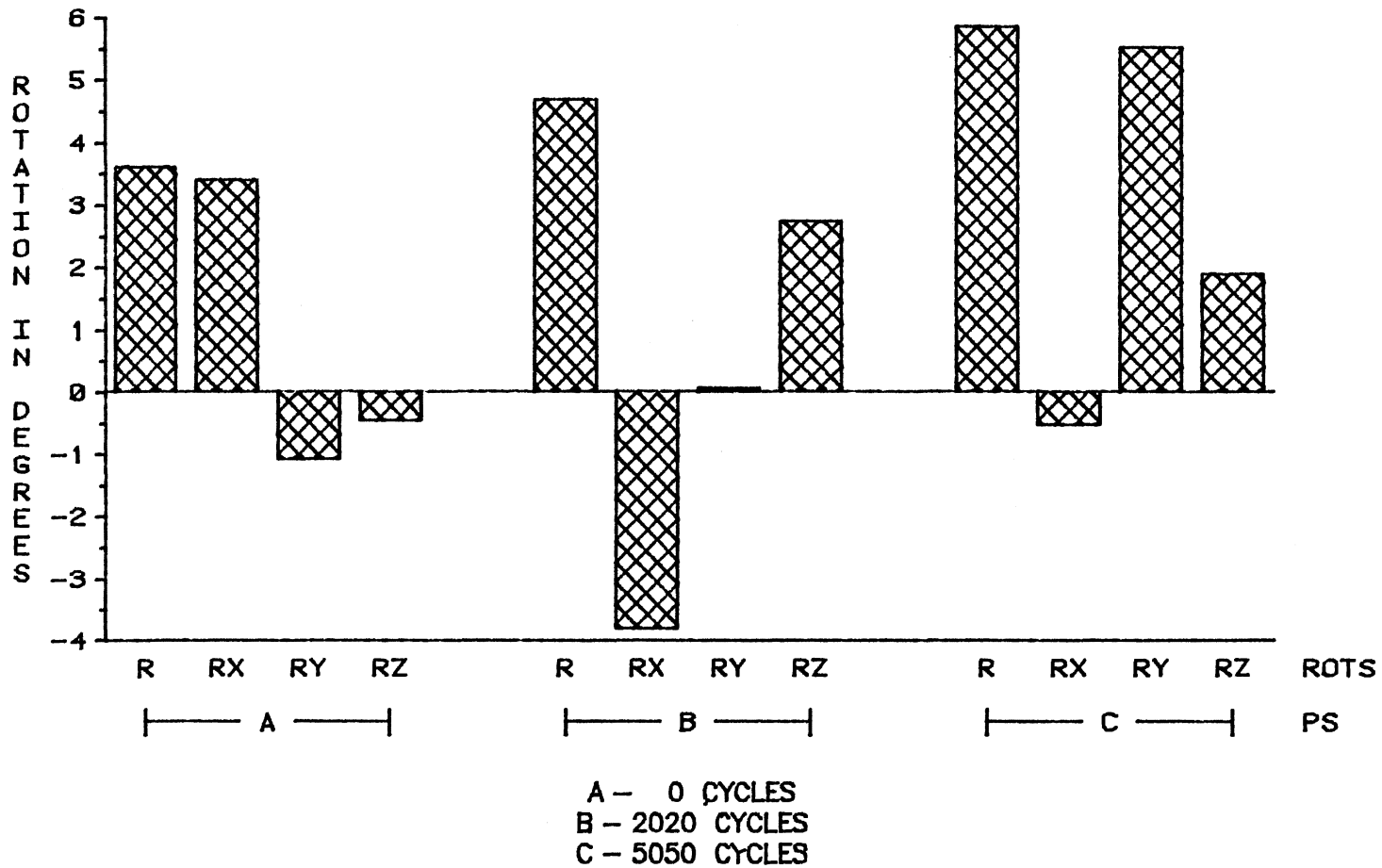


Figure 18. Rotations Under Positive Shear (0 deg.) Under Torsional Fatigue Load

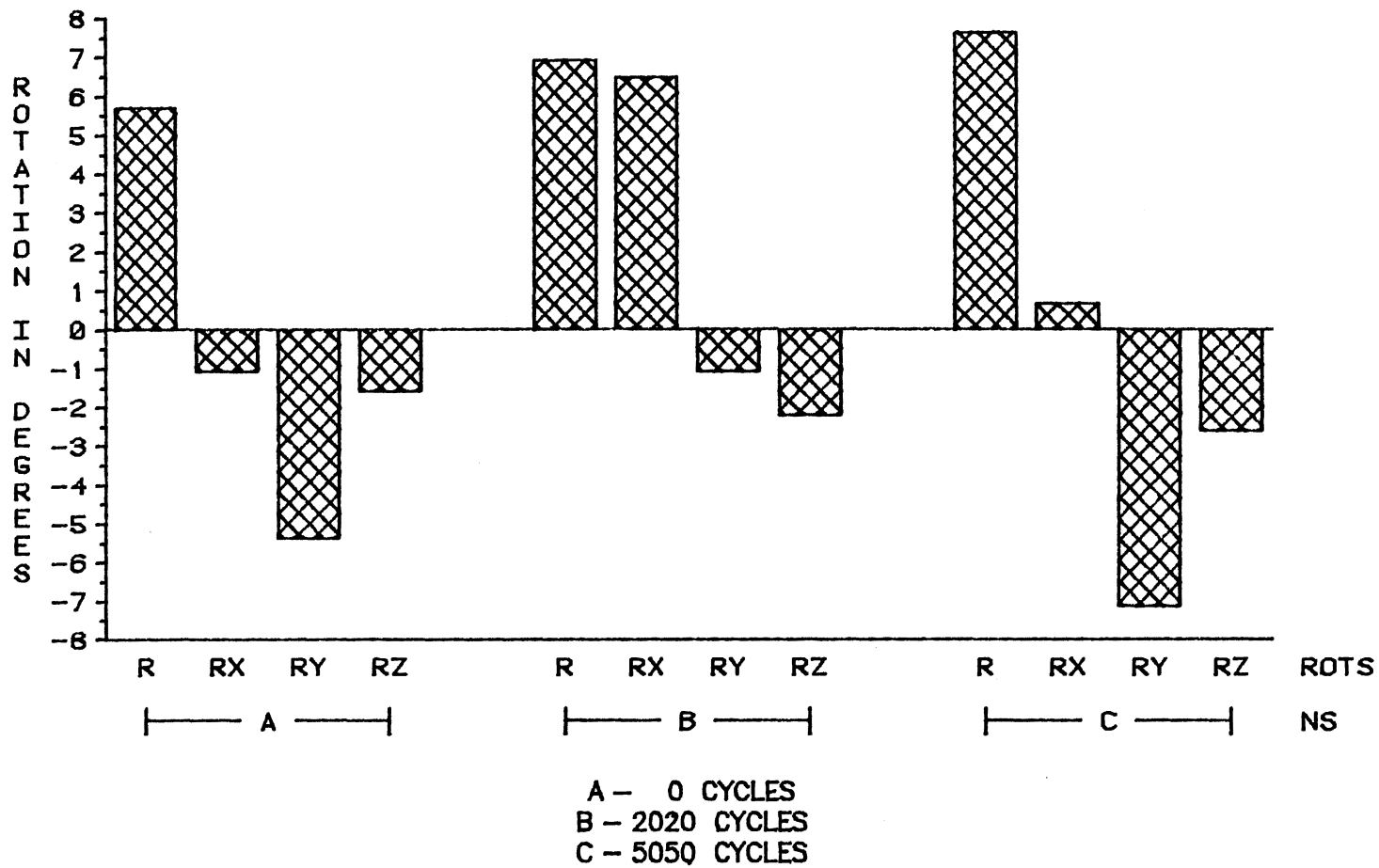


Figure 19. Rotations Under Negative Shear (0 deg.) Under Torsional Fatigue Load

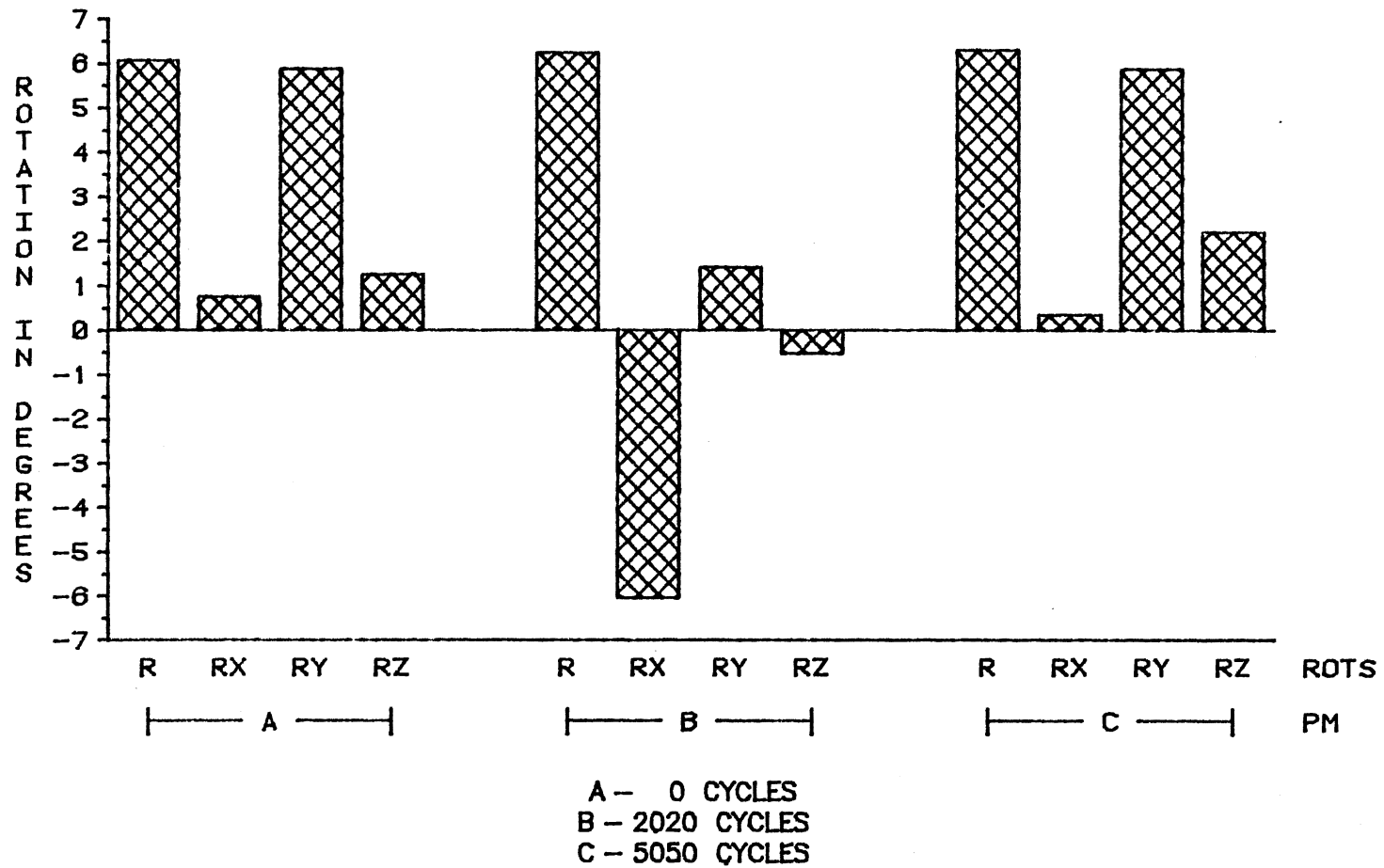


Figure 20. Rotations Under Positive Moment (0 deg.) Under Torsional Fatigue Load

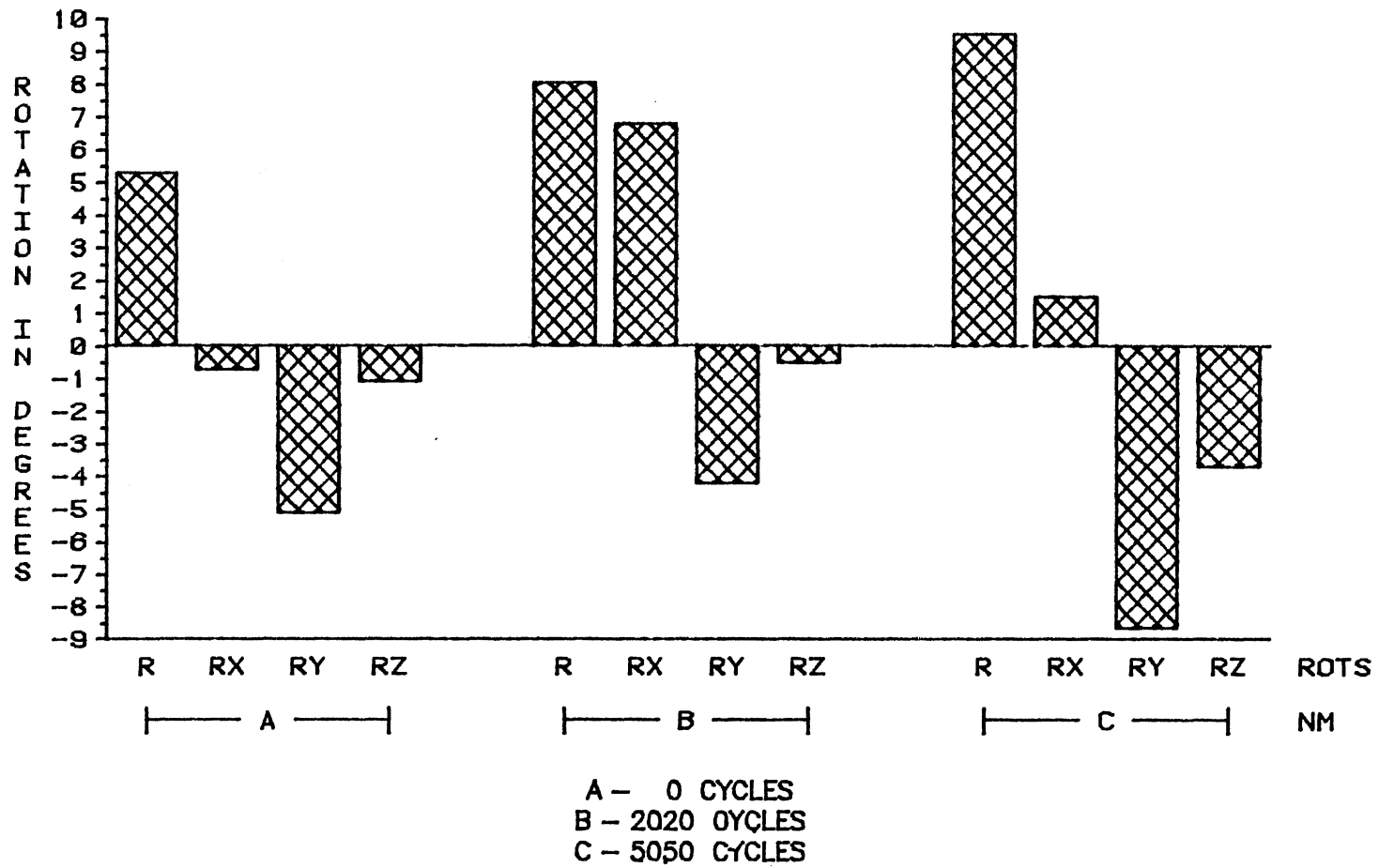


Figure 21. Rotations Under Negative Moment (0 deg.) Under Torsional Fatigue Load

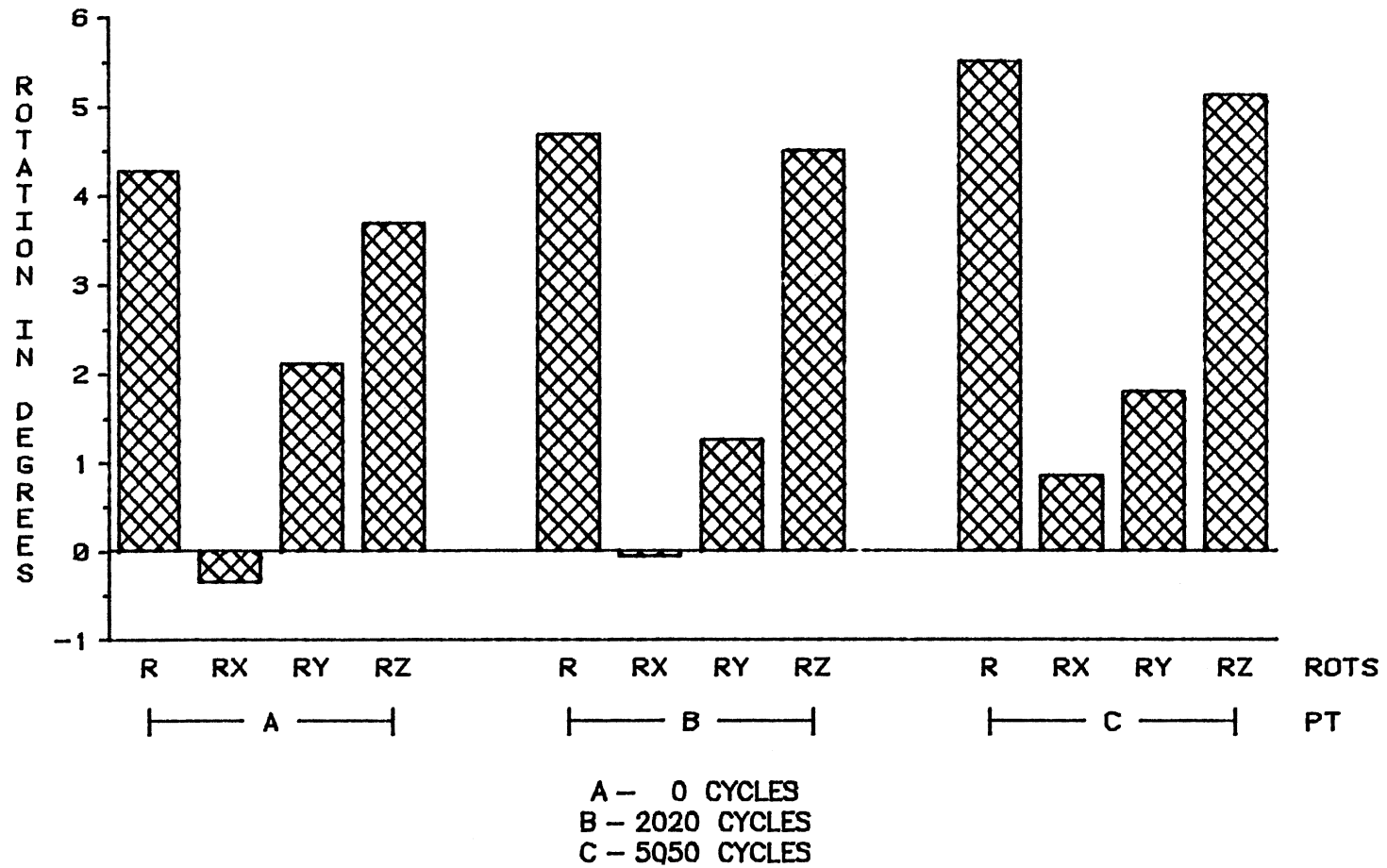


Figure 22. Rotations Under Positive Torque Under Torsional Fatigue Load

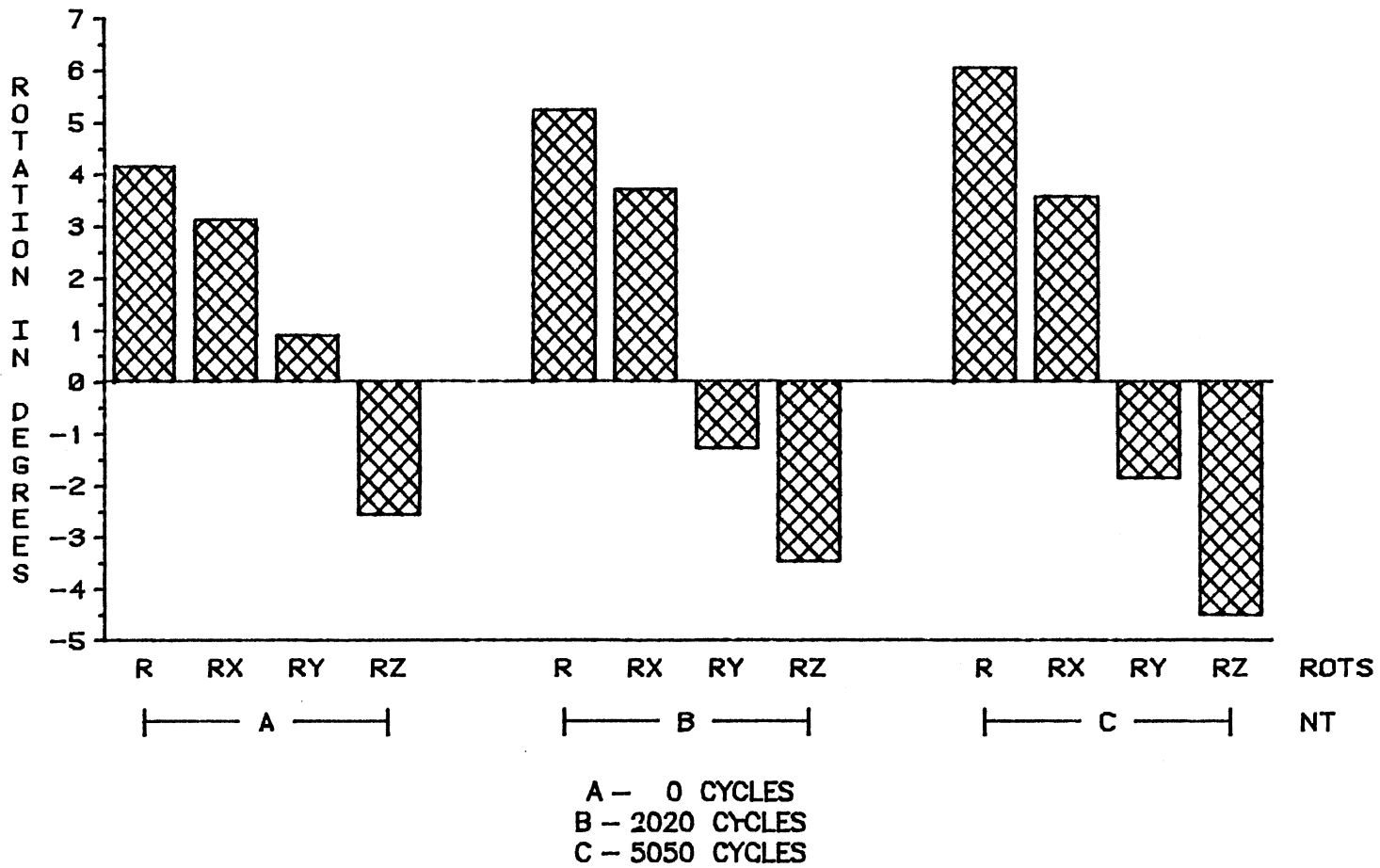
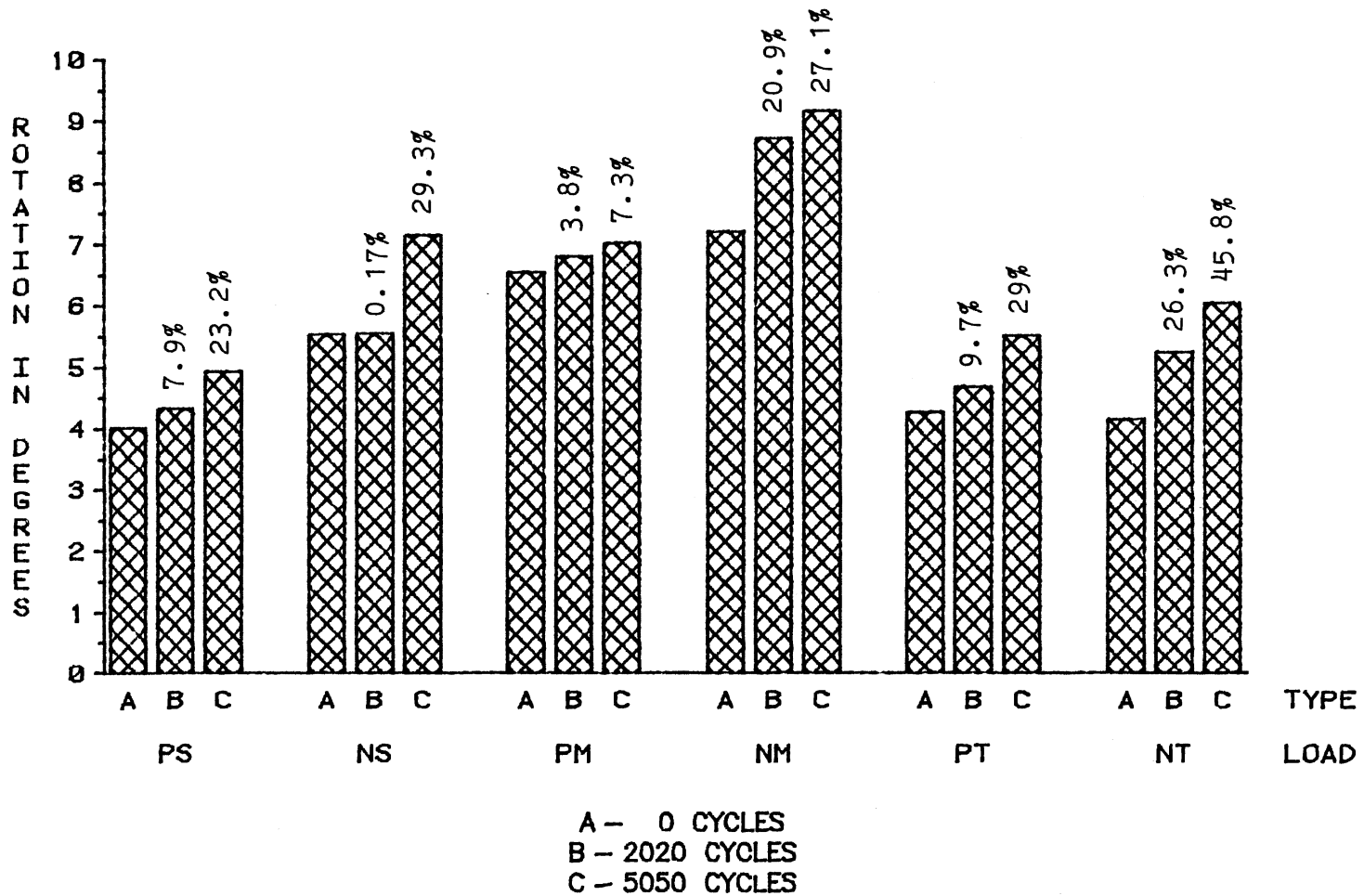


Figure 23. Rotations Under Negative Torque Under Torsional Fatigue Load



A - 0 CYCLES  
 B - 2020 CYCLES  
 C - 5050 CYCLES  
 Percentage increase with respect to  
 0 cycles is indicated on the top of each bar

Figure 24. Rotations for Different Loads (90 deg.) Under Torsional Fatigue Load

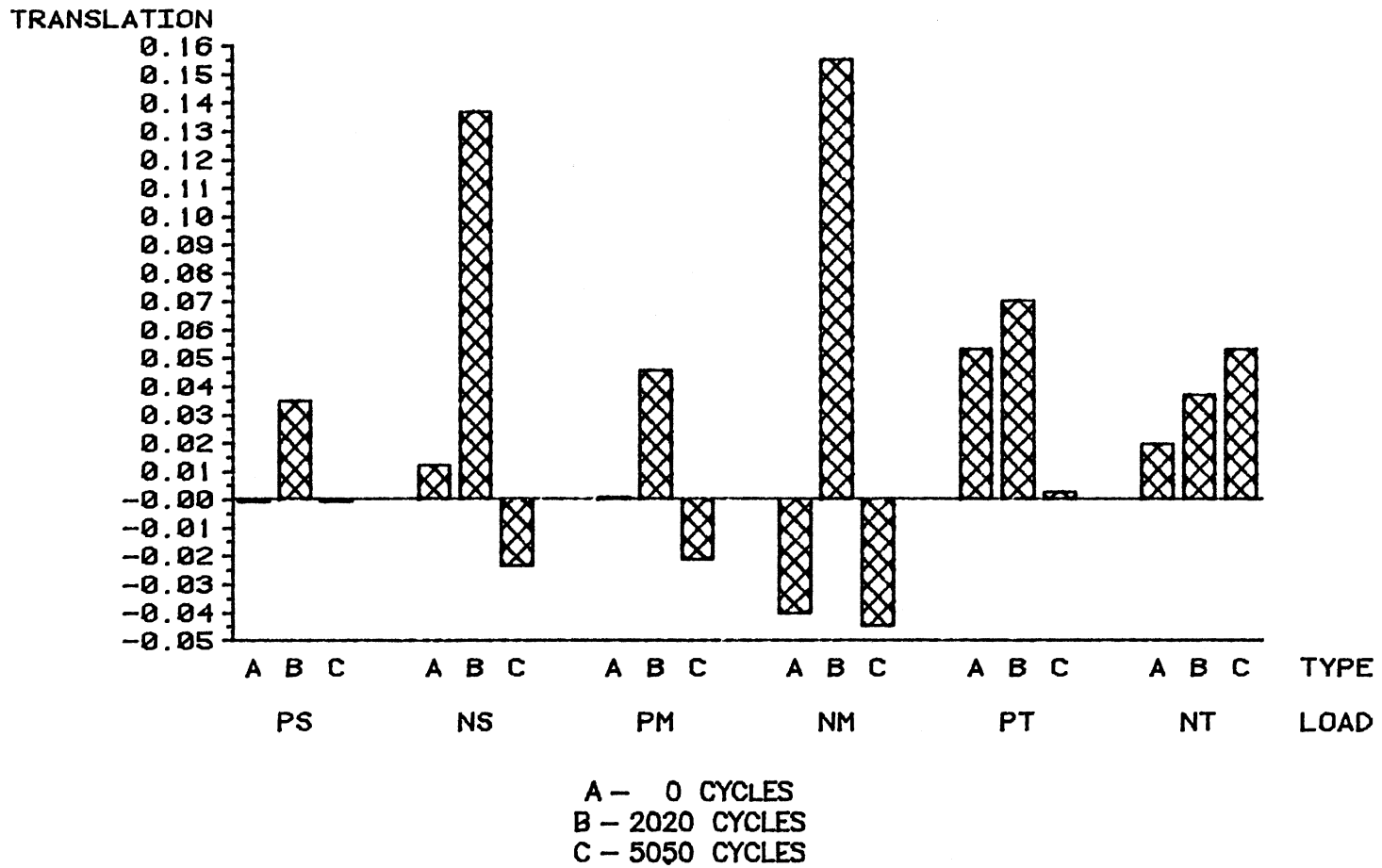


Figure 25. Translations for Different Loads (90 deg.) Under Torsional Fatigue Load



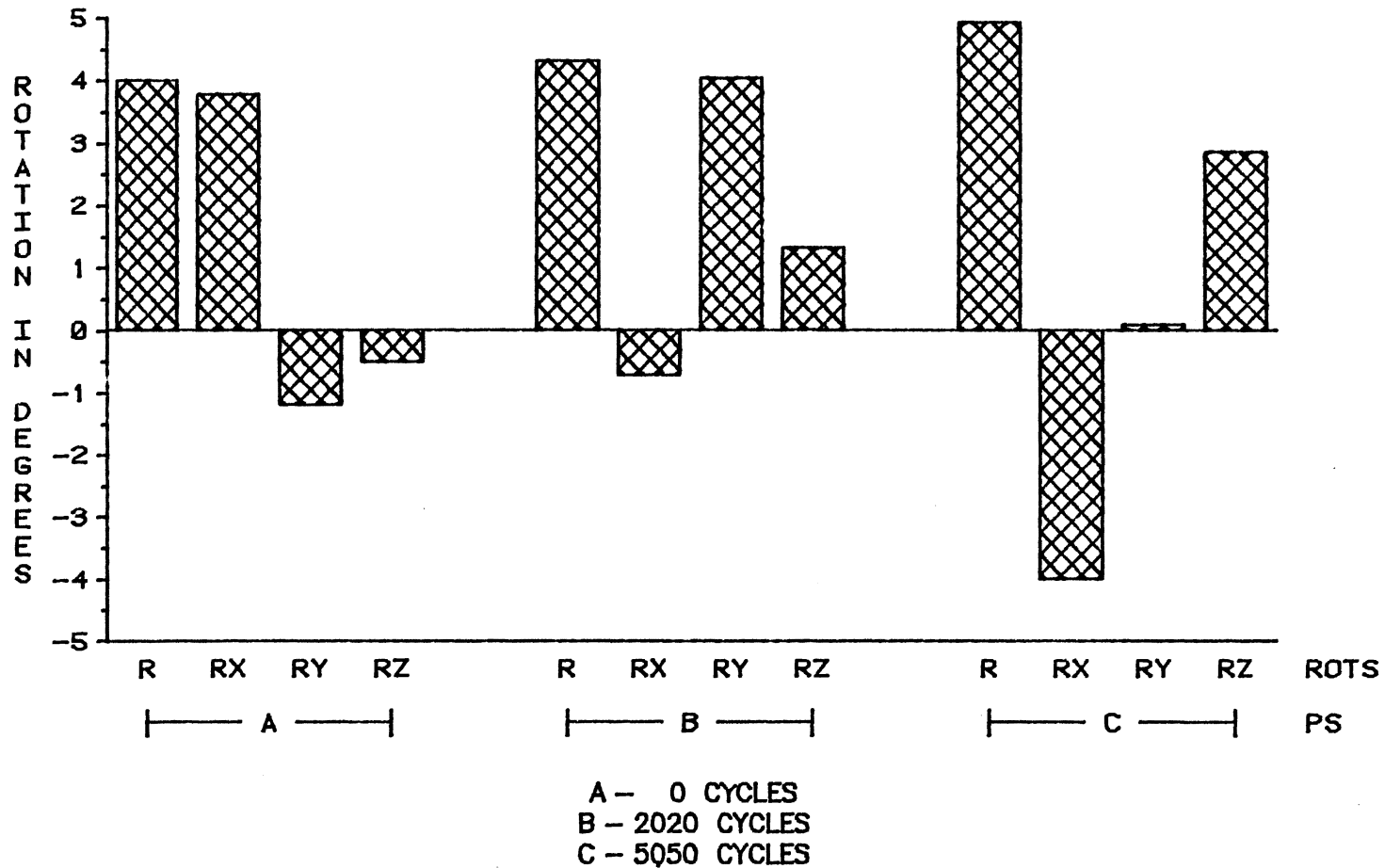


Figure 26. Rotations Under Positive Shear (90 deg.) Under Torsional Fatigue Load

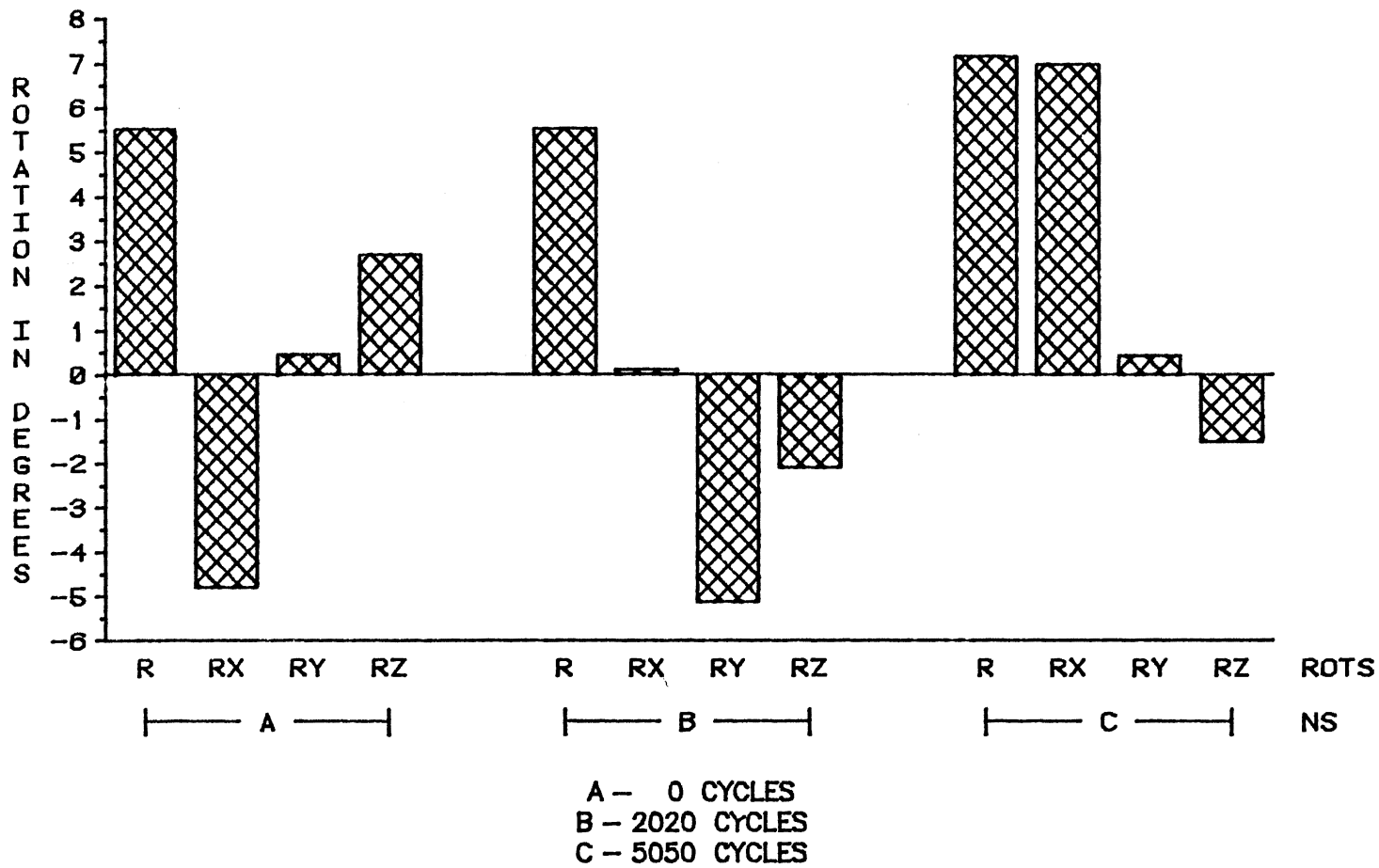


Figure 27. Rotations Under Negative Shear (90 deg.) Under Torsional Fatigue Load

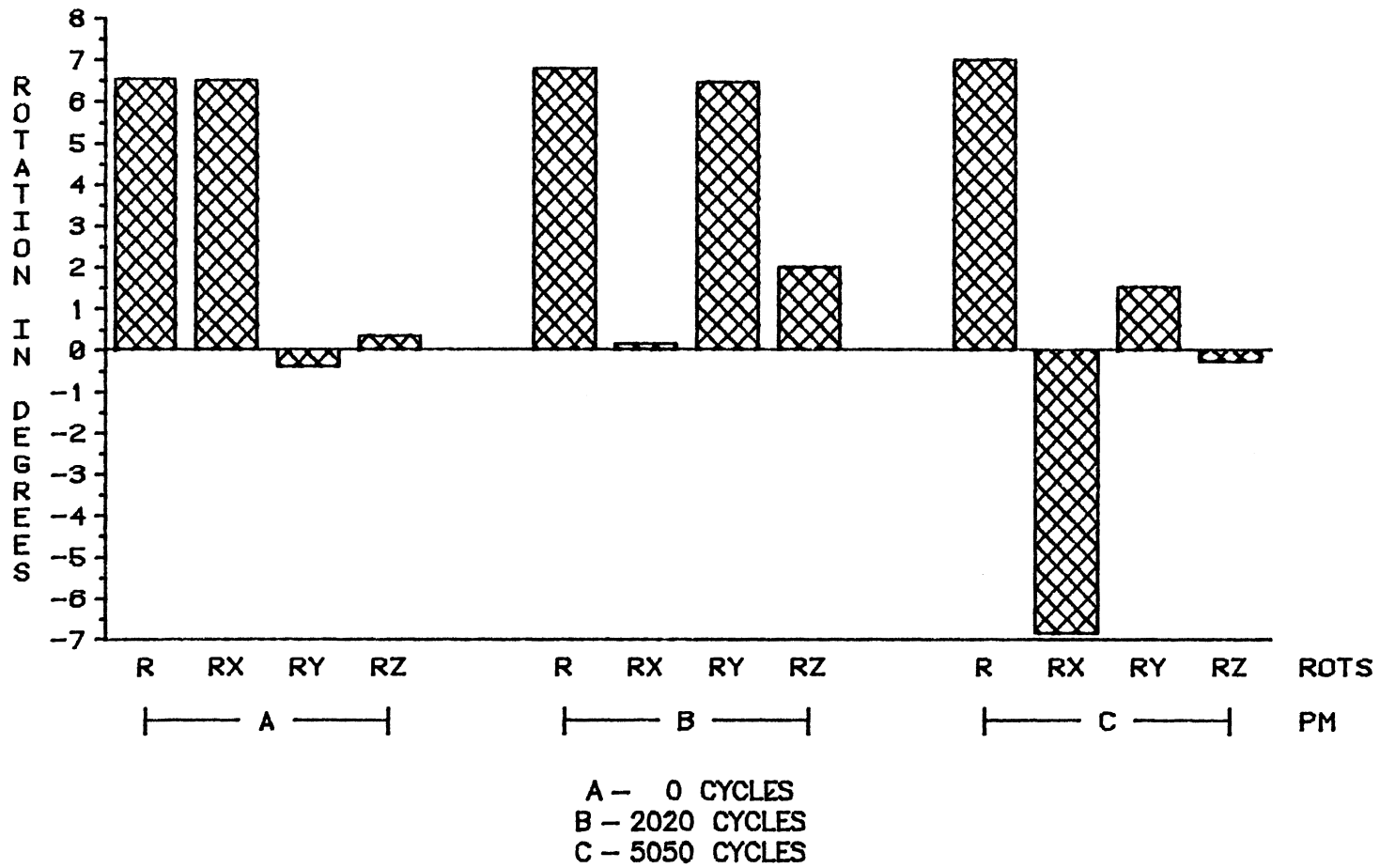


Figure 28. Rotations Under Positive Moment (90 deg.) Under Torsional Fatigue Load

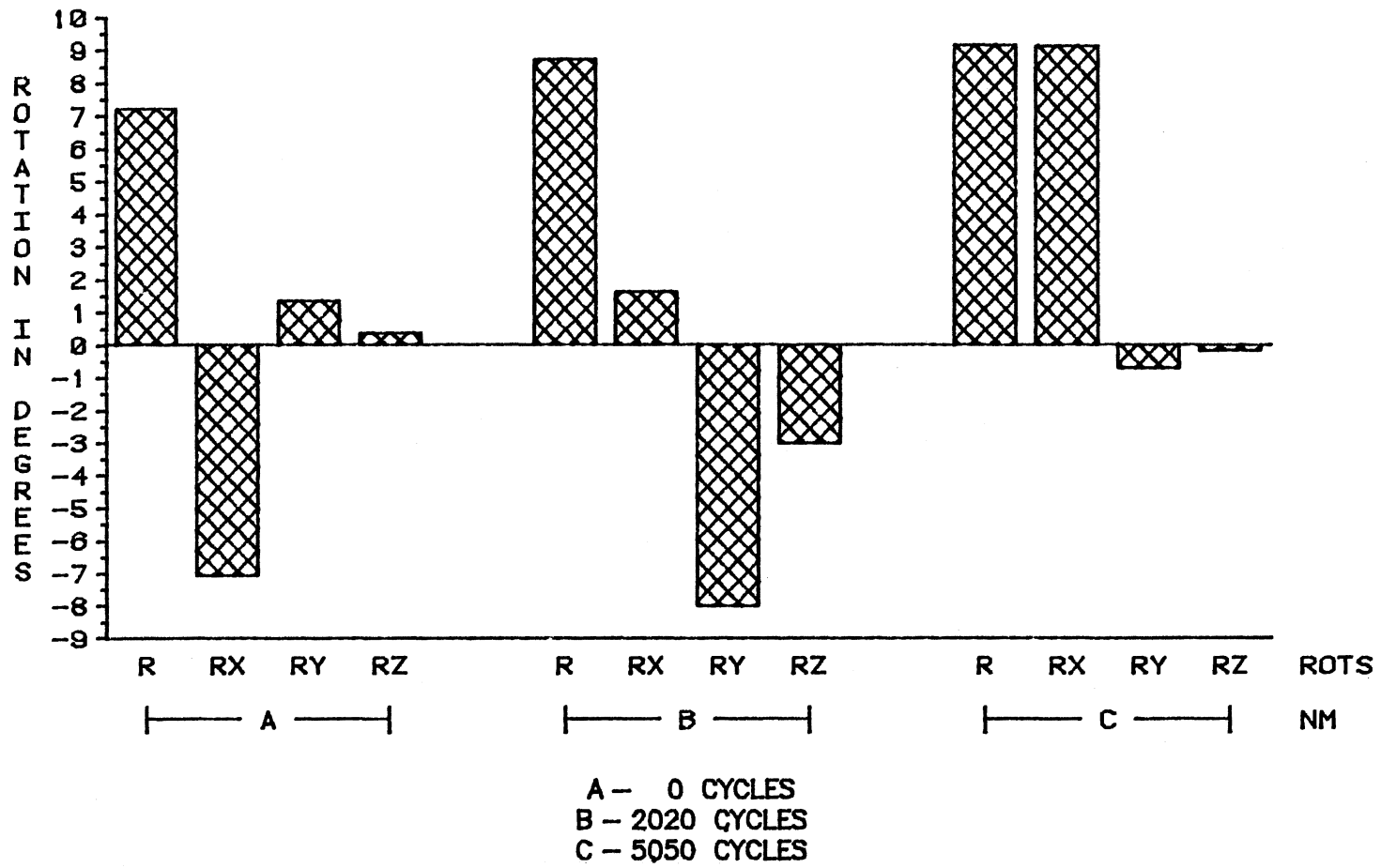
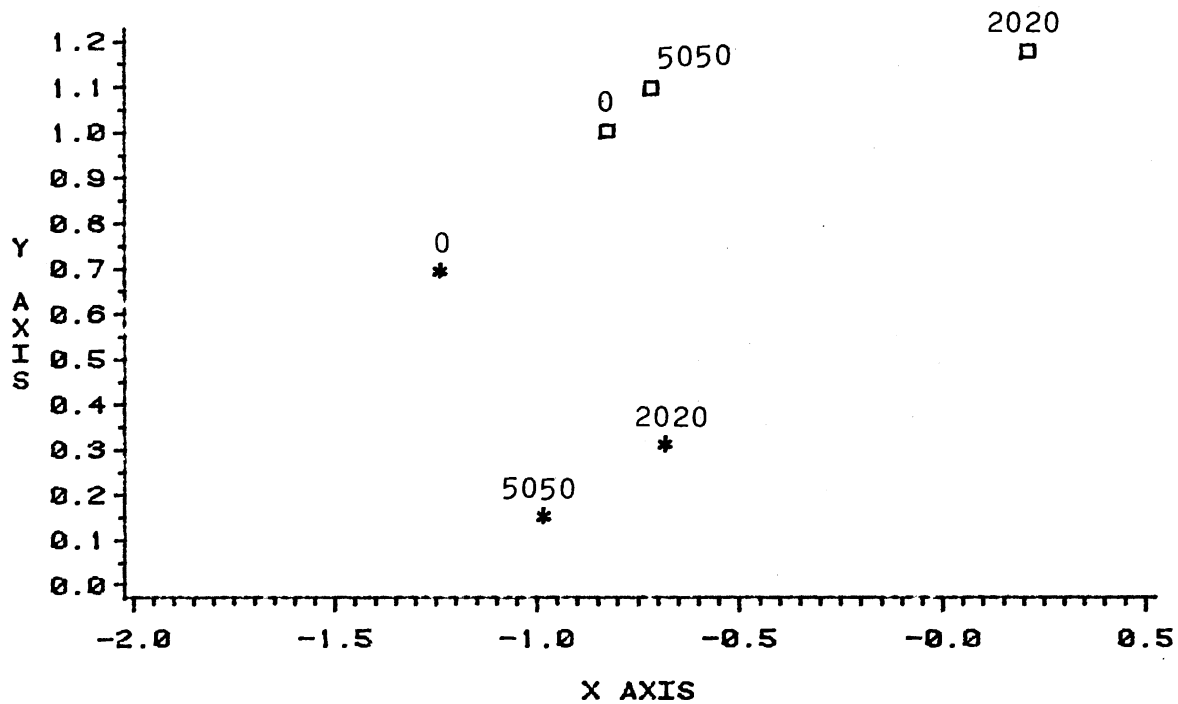
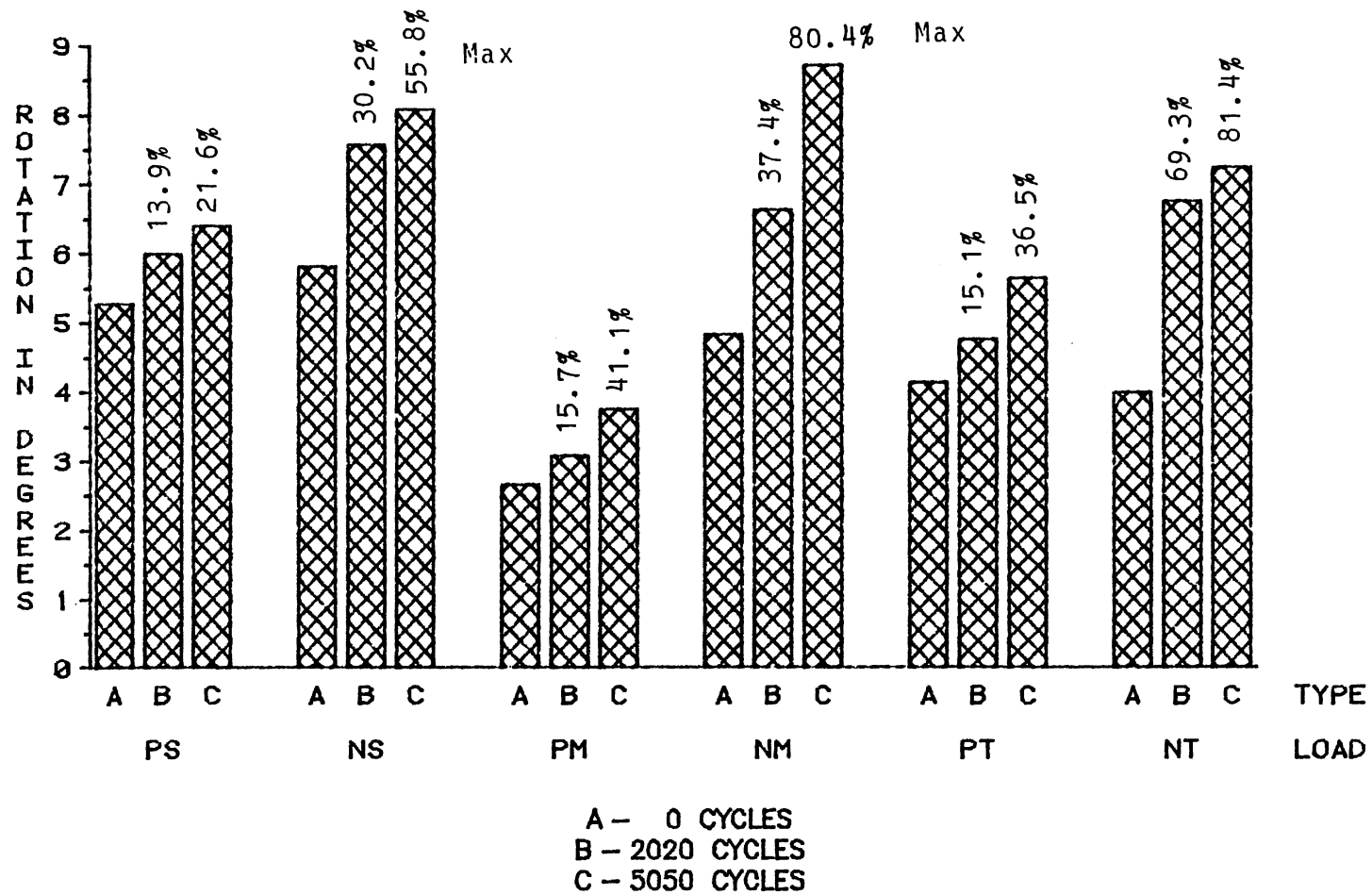


Figure 29. Rotations Under Negative Moment (90 deg.) Under Torsional Fatigue Load



\* REPRESENTS POINTS FOR POSITIVE TORQUE  
 □ REPRESENTS POINTS FOR NEGATIVE TORQUE

Figure 30. Points of Intersection of the Screw Axis With XY Plane for PT and NT Loads Under Torsional Fatigue Load



Percentage increase with respect to 0 cycles is indicated on the top of each bar

Figure 31. Rotations for Different Loads (0 deg.) Under Bending Fatigue Load

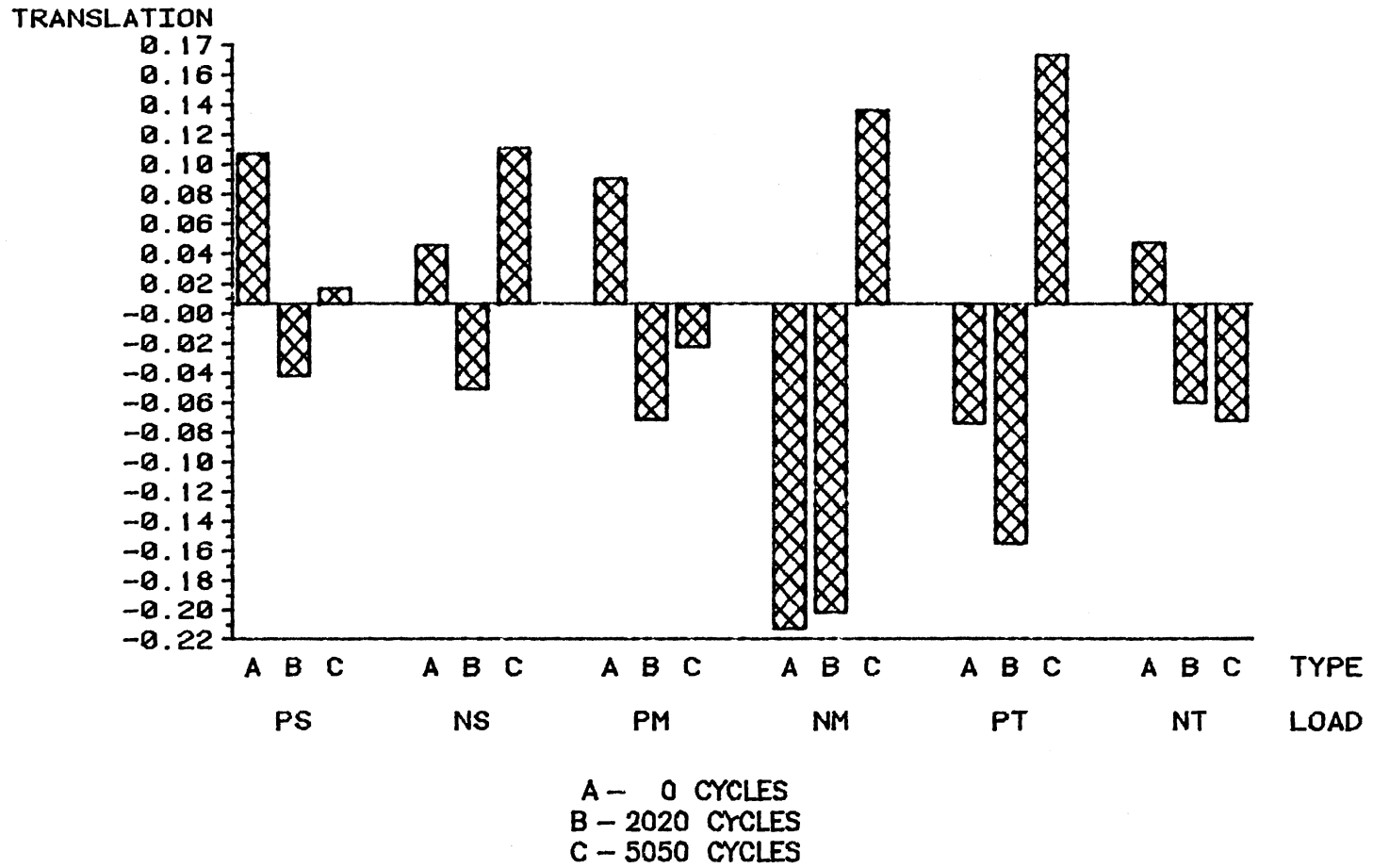


Figure 32. Translations for Different Loads (0 deg.) Under Bending Fatigue Load

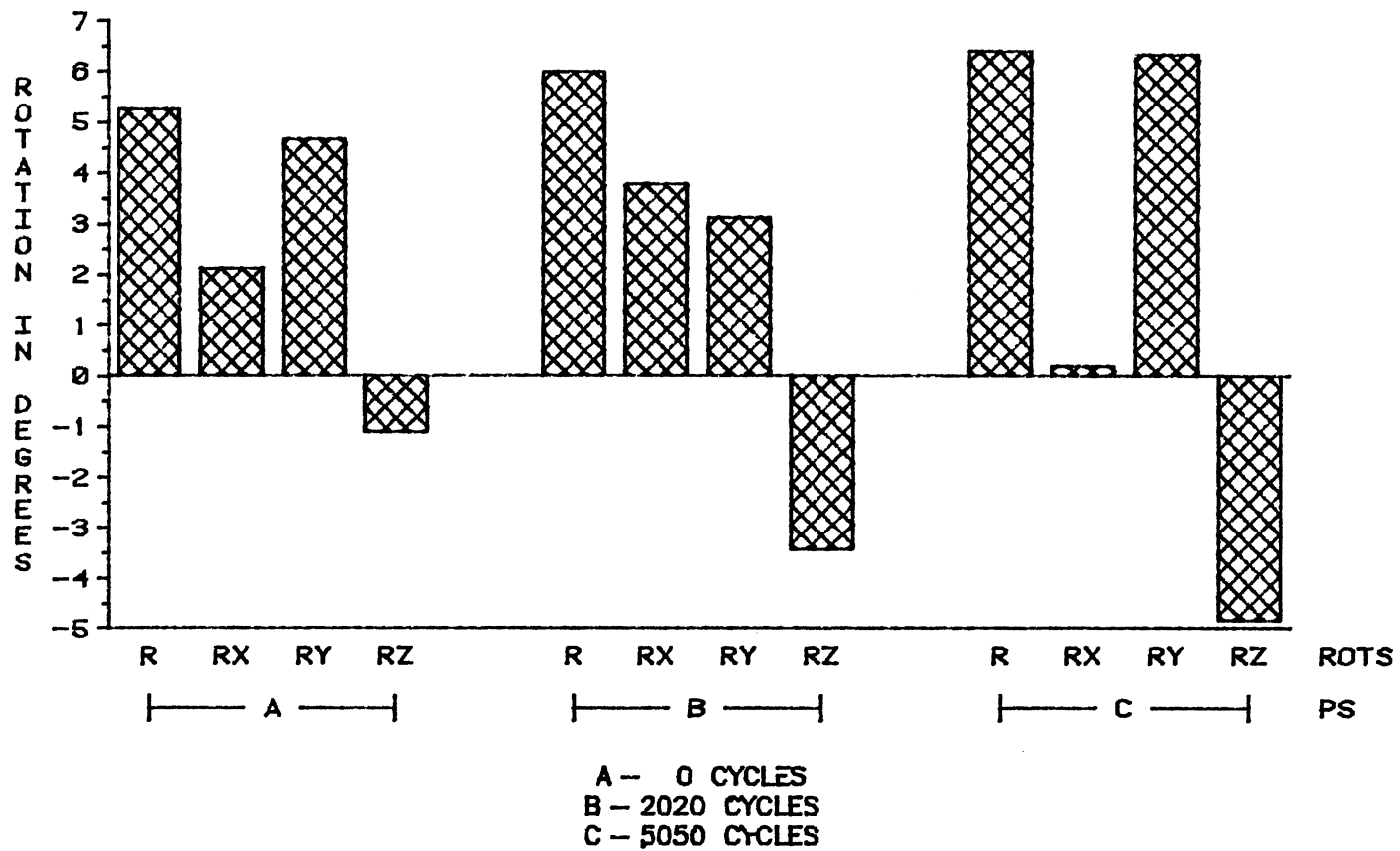


Figure 33. Rotations Under Positive Shear (0 deg.) Under Bending Fatigue Load



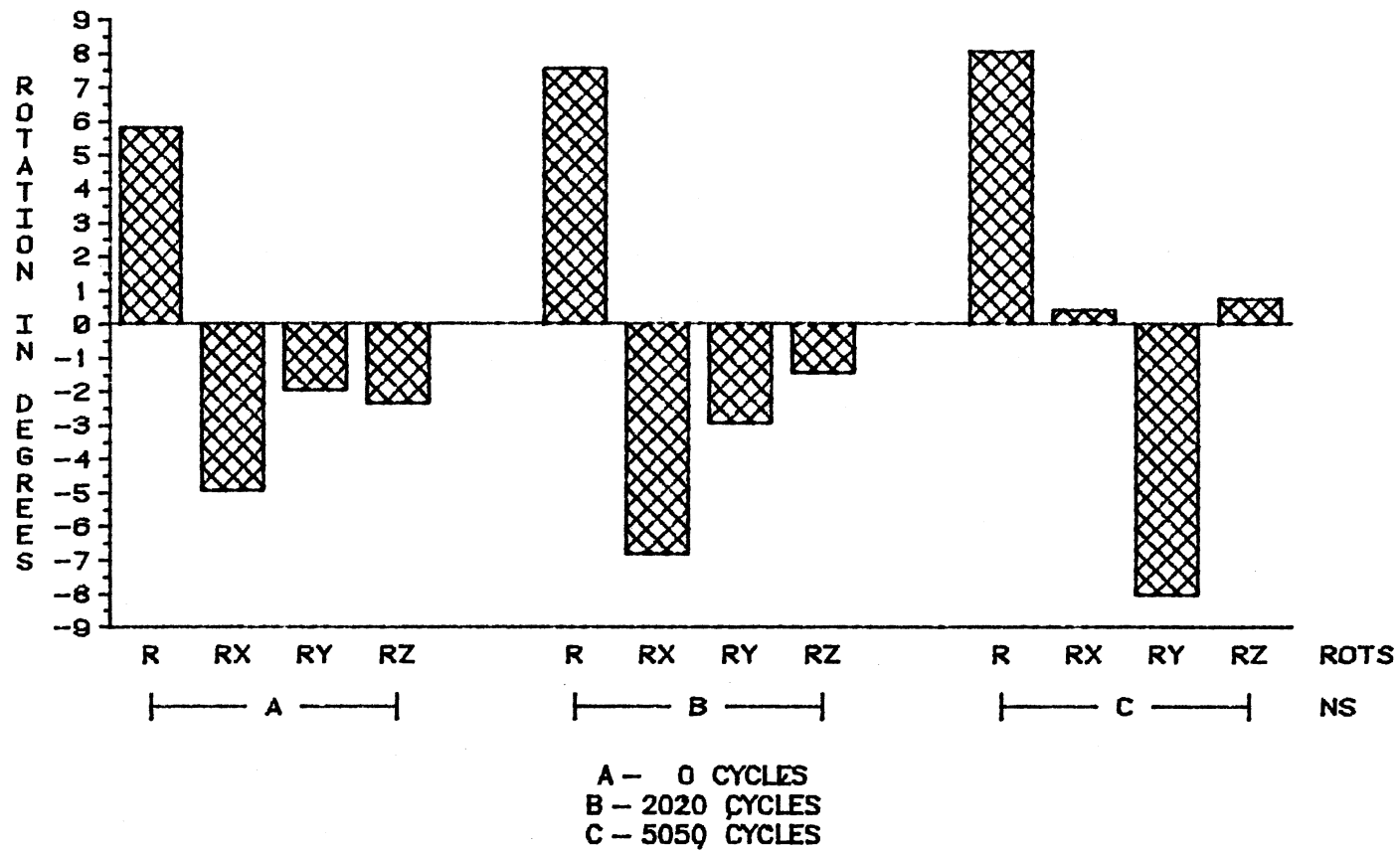


Figure 34. Rotations Under Negative Shear (0 deg.) Under Bending Fatigue Load

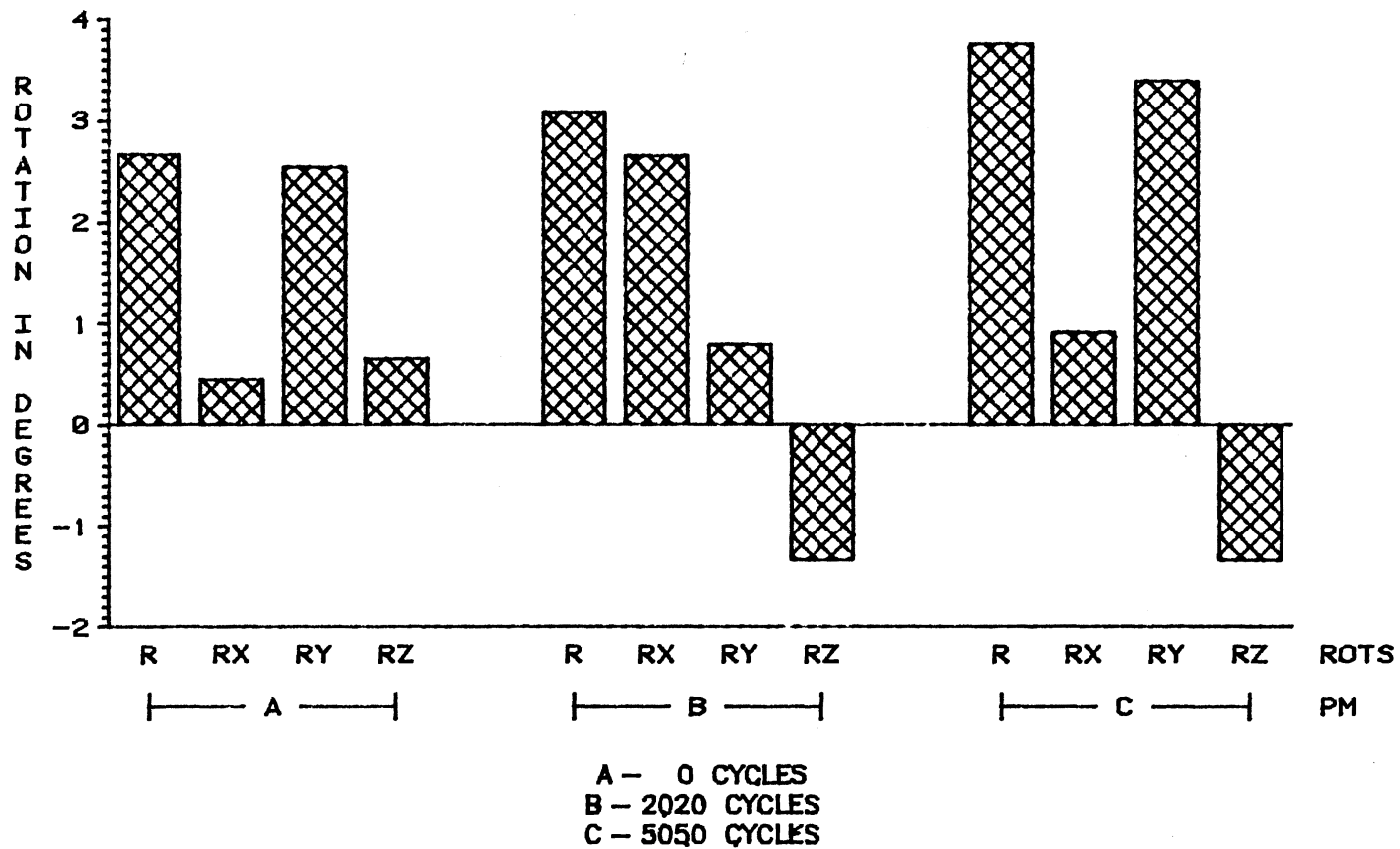


Figure 35. Rotations Under Positive Moment (0 deg.) Under Bending Fatigue Load

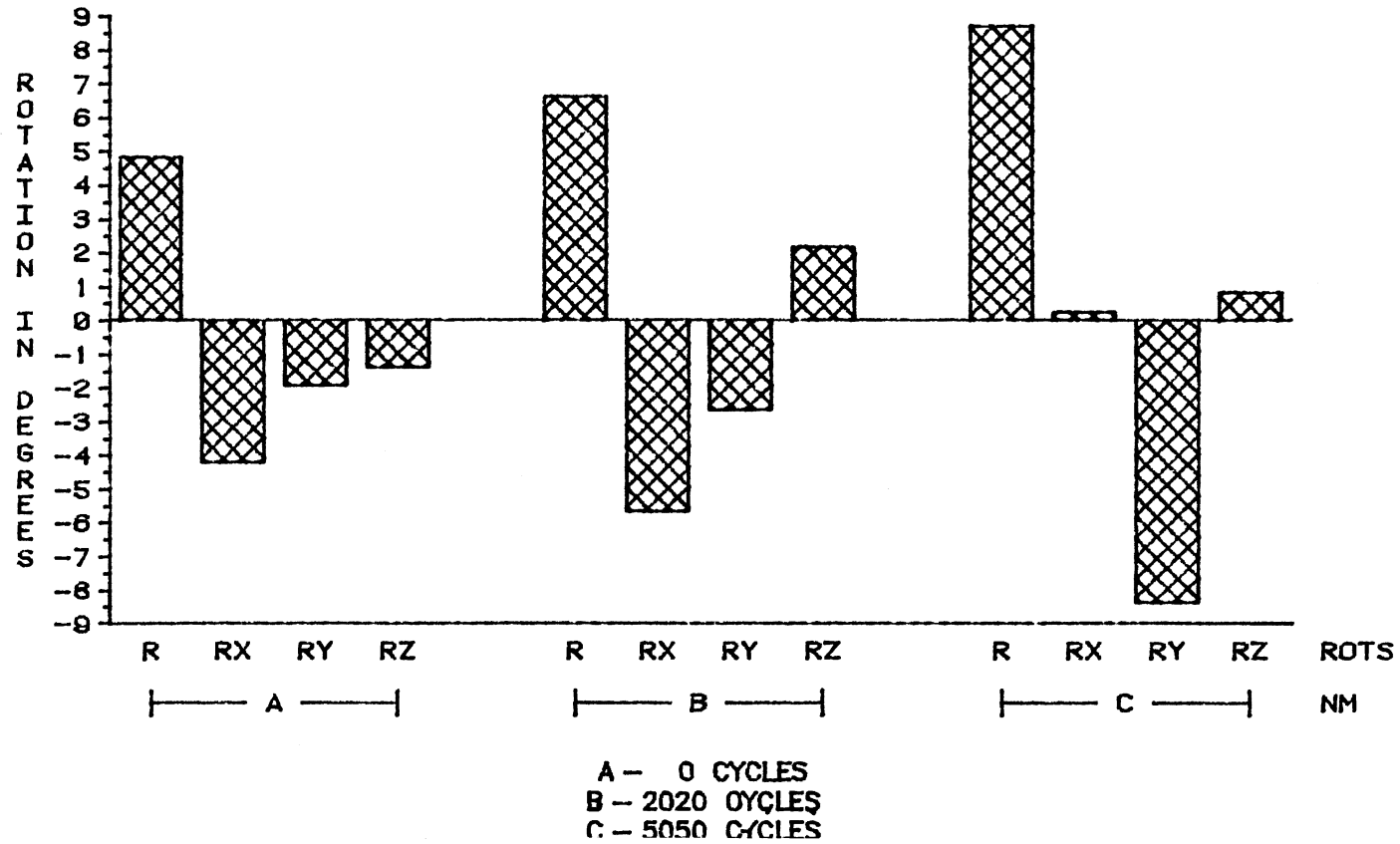


Figure 36. Rotations Under Negative Moment (0 deg.) Under Bending Fatigue Load

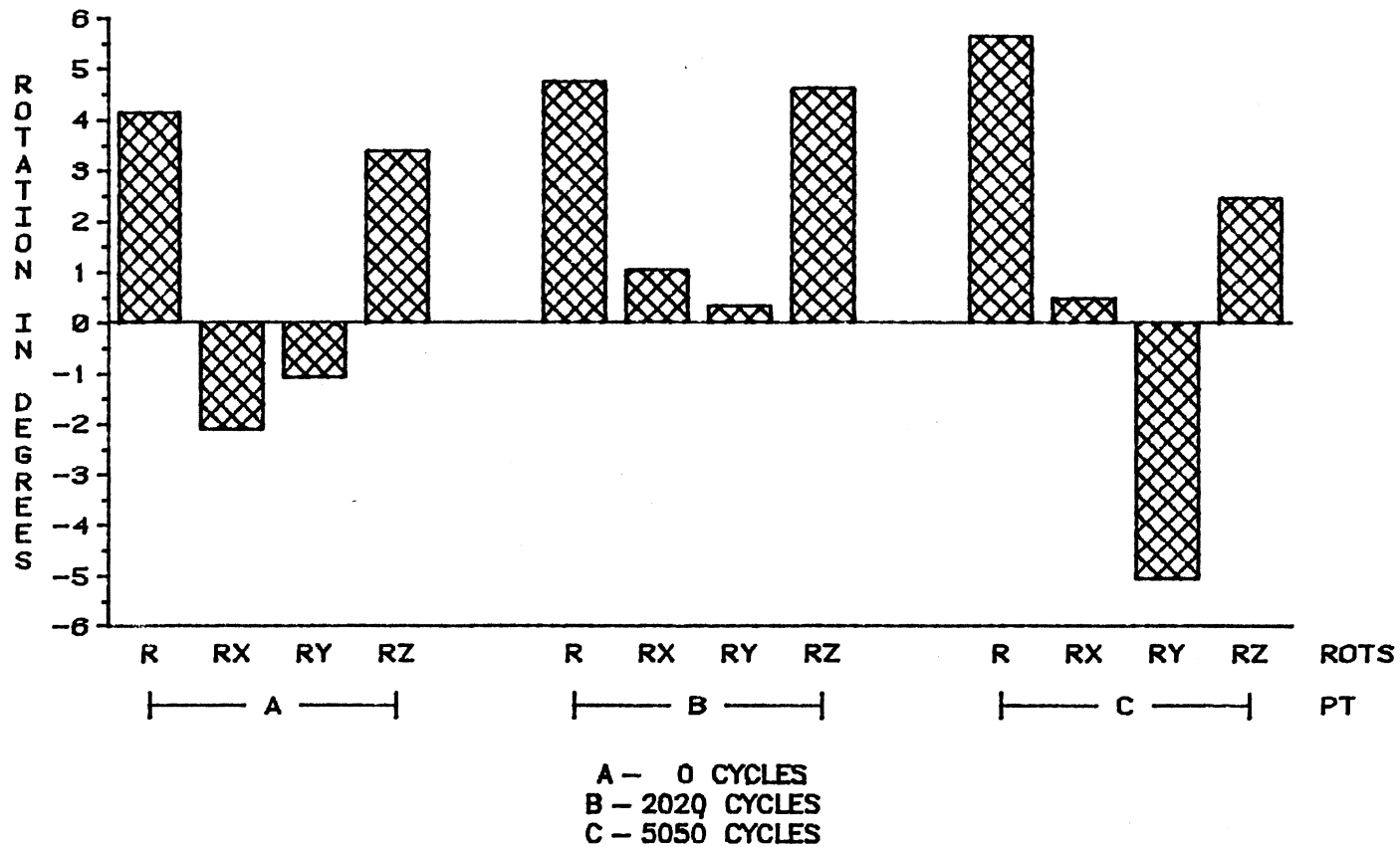


Figure 37. Rotations Under Positive Torque Under Bending Fatigue Load

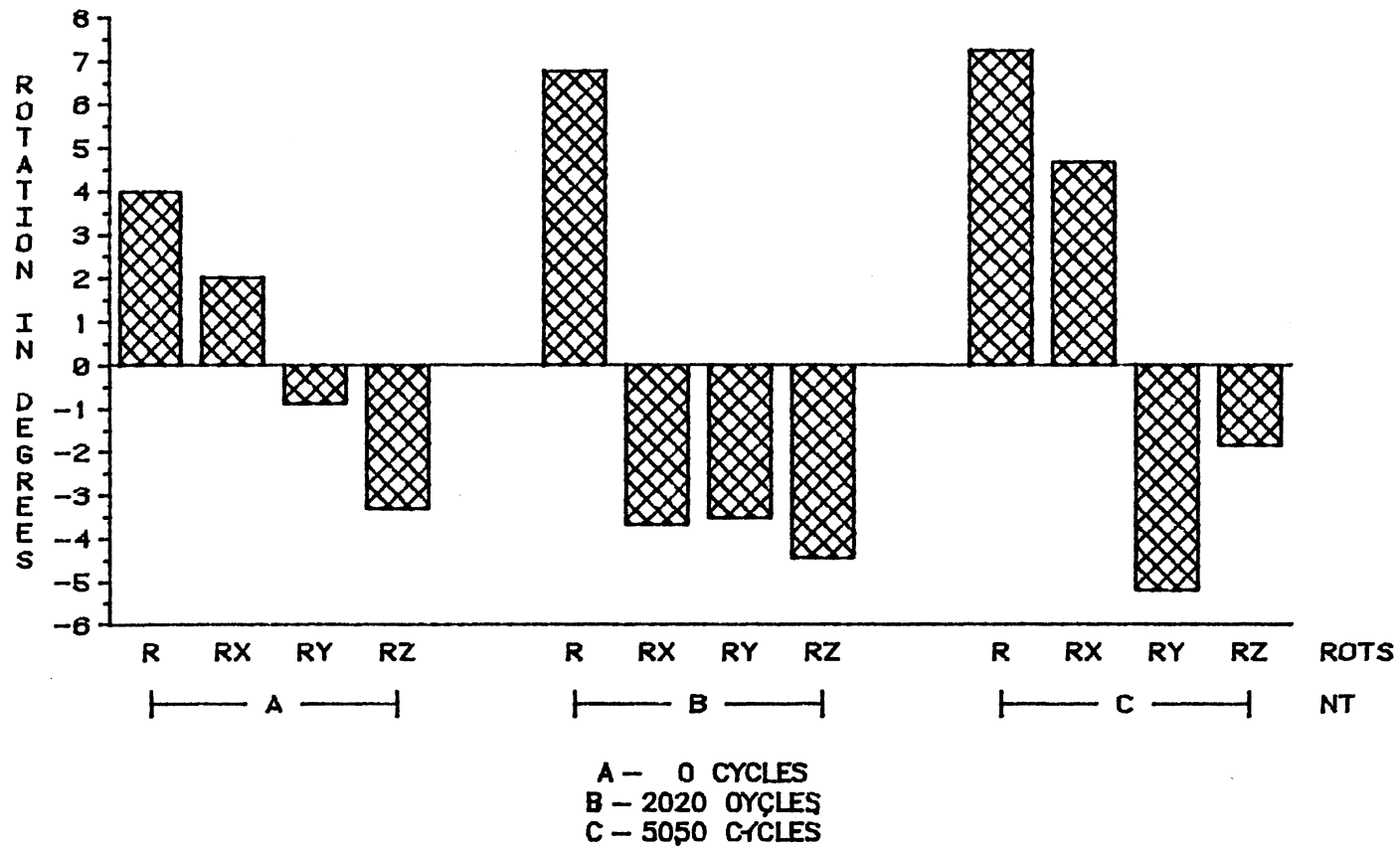
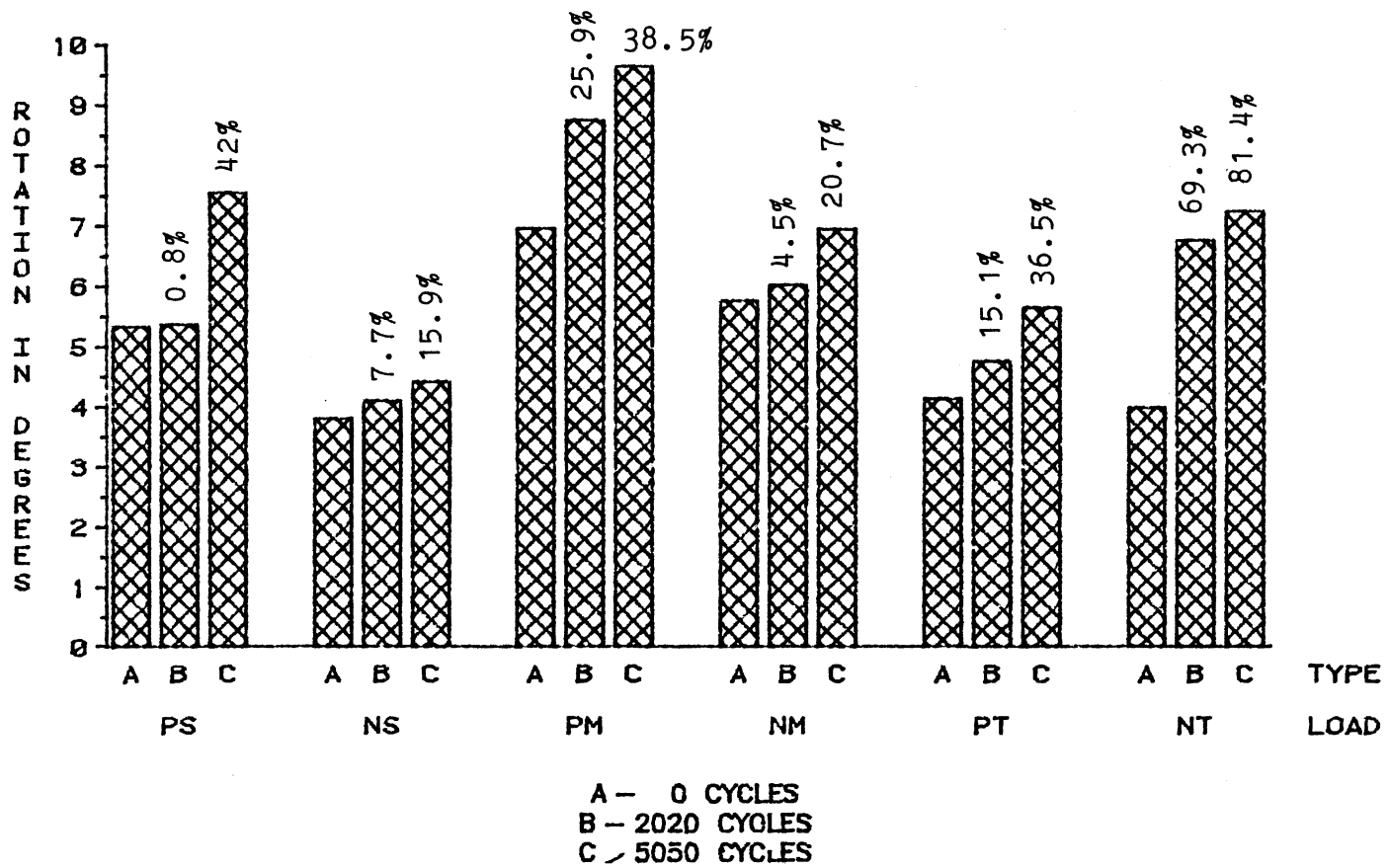


Figure 38. Rotations Under Negative Torque Under Bending Fatigue Load



Percentage increase with respect to 0 cycles is indicated on the top of each bar

Figure 39. Rotations for Different Loads (90 deg.) Under Bending Fatigue Load

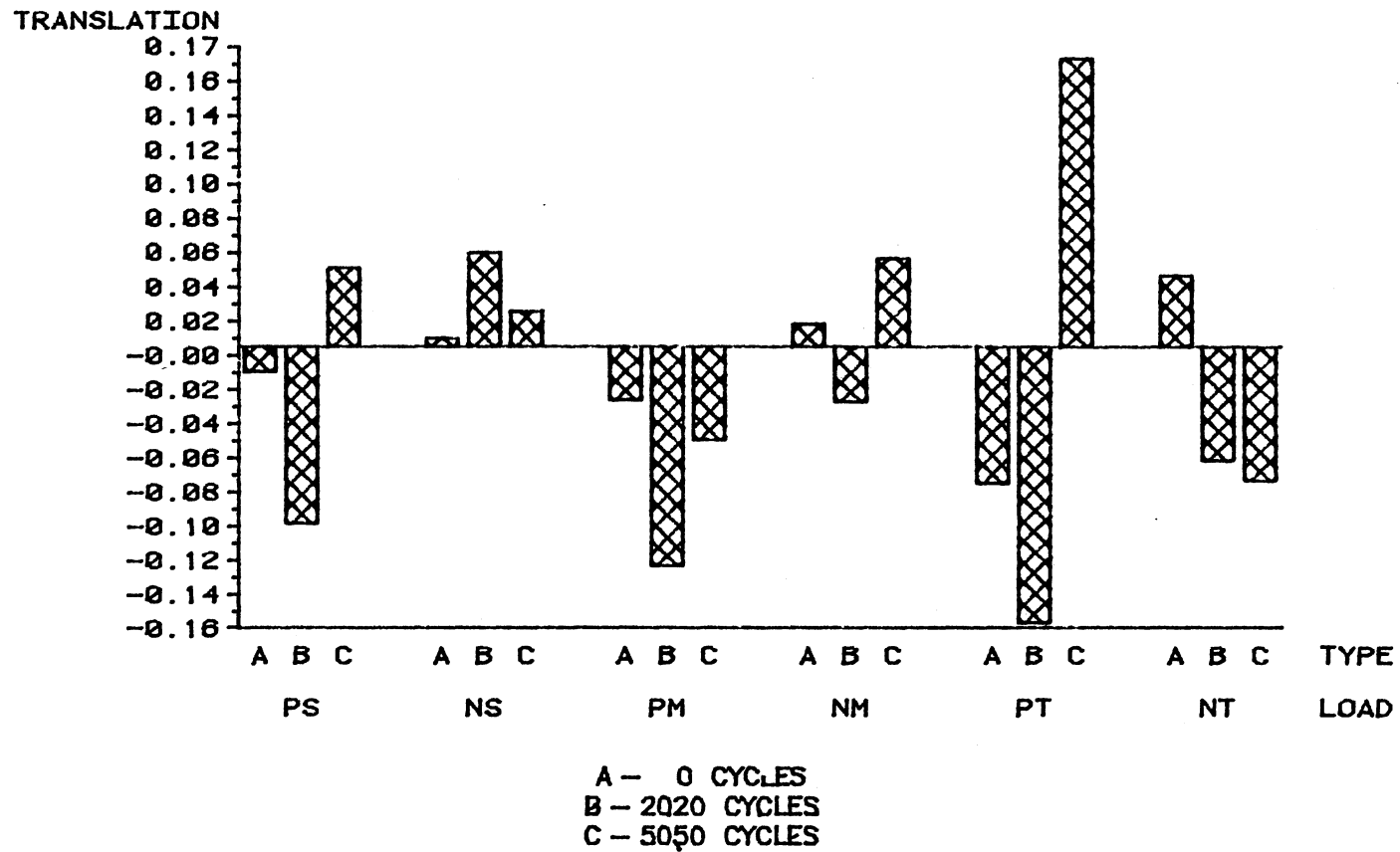


Figure 40. Translations for Different Loads (90 deg.) Under Bending Fatigue Load

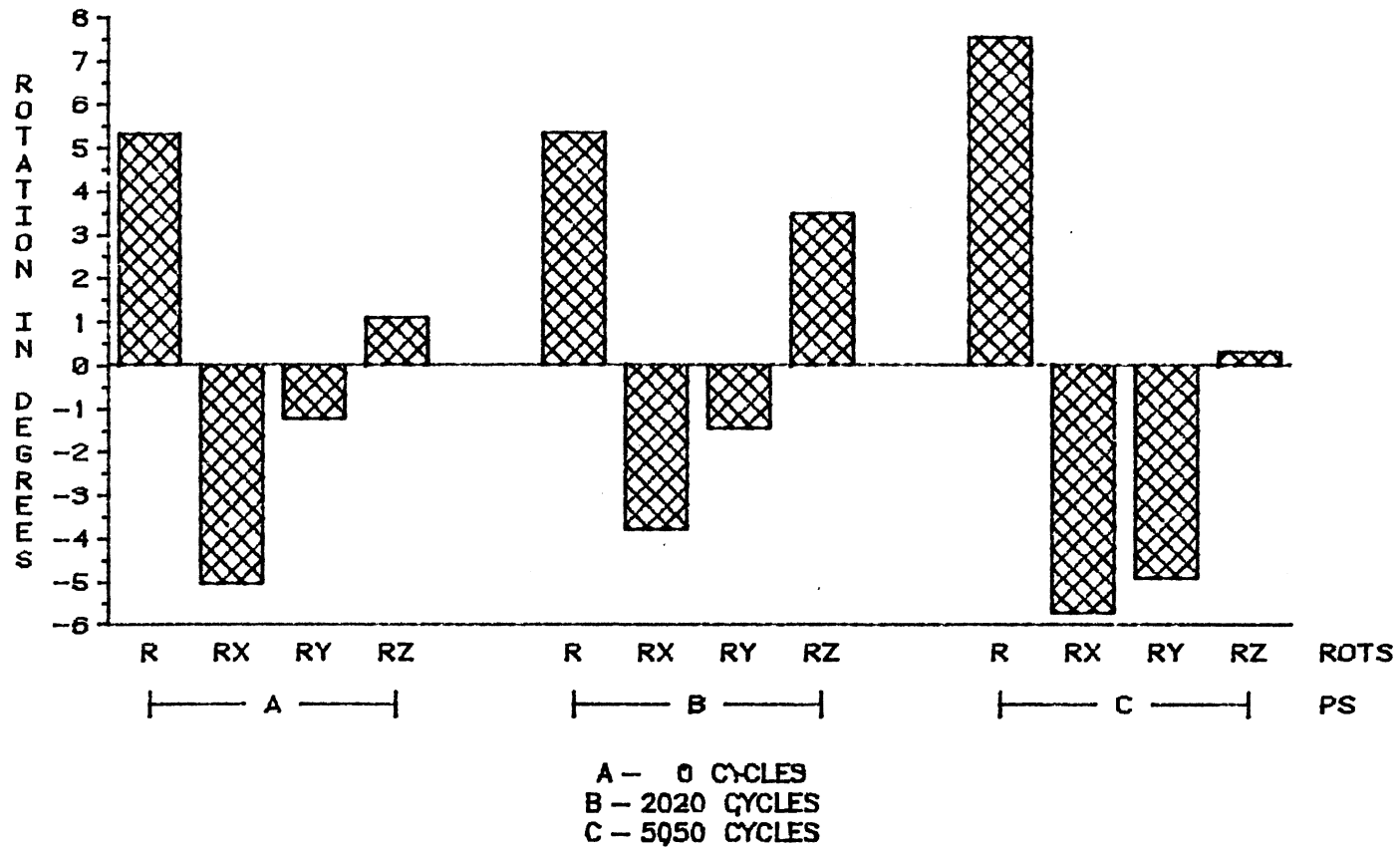


Figure 41. Rotations Under Positive Shear (90 deg.) Under Bending Fatigue Load



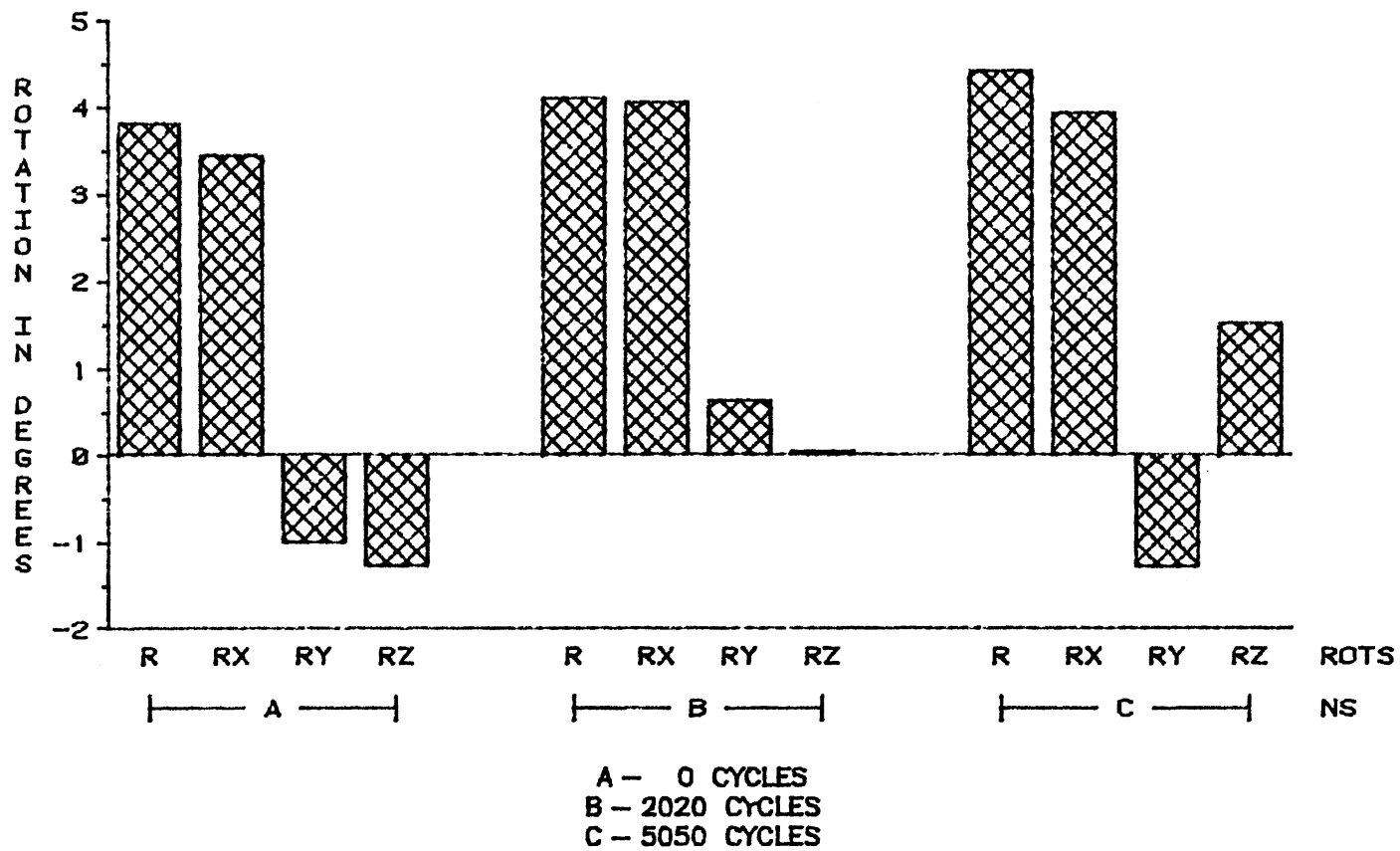


Figure 42. Rotations Under Negative Shear (90 deg.) Under Bending Fatigue Load

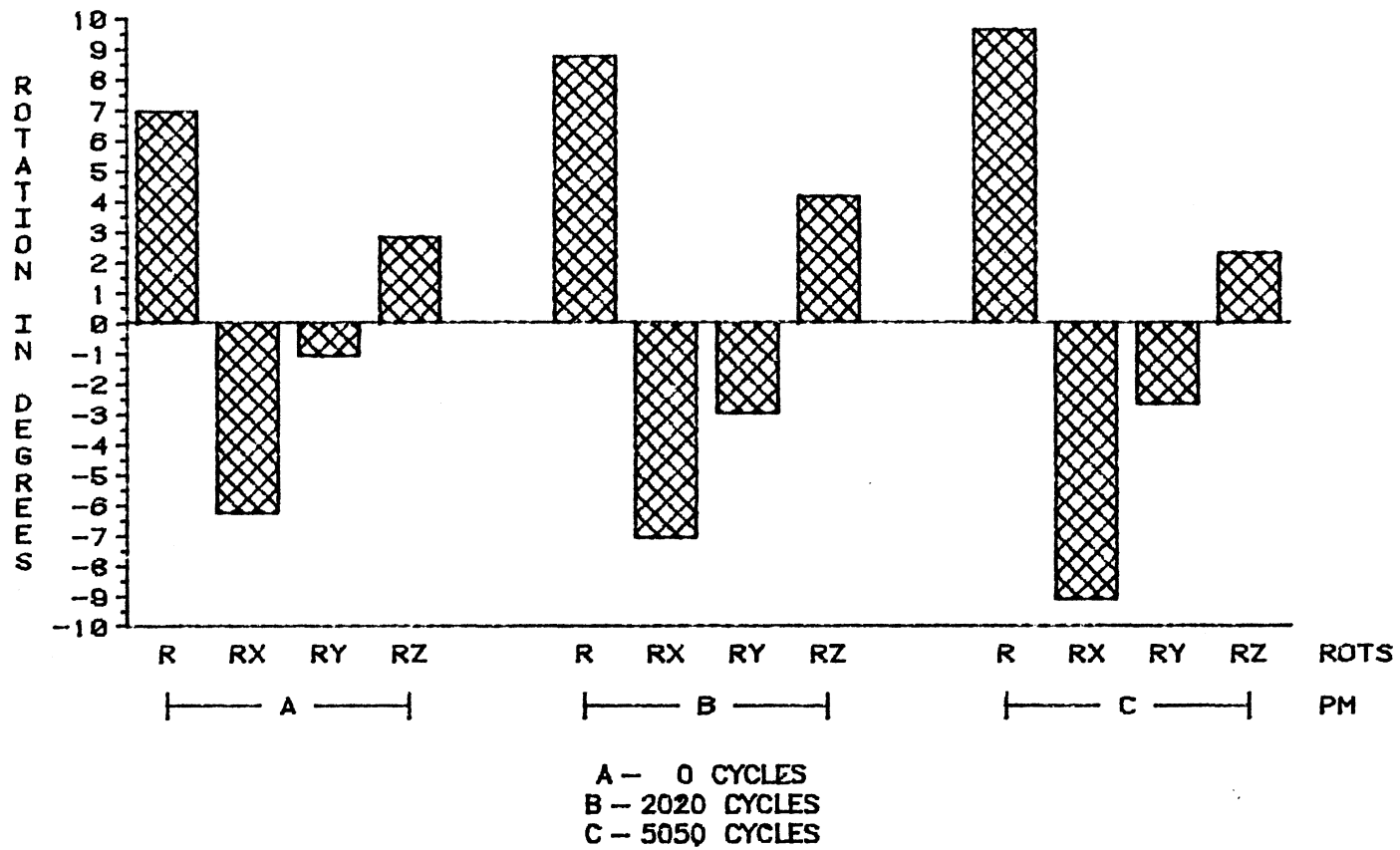


Figure 43. Rotations Under Positive Moment (90 deg.) Under Bending Fatigue Load

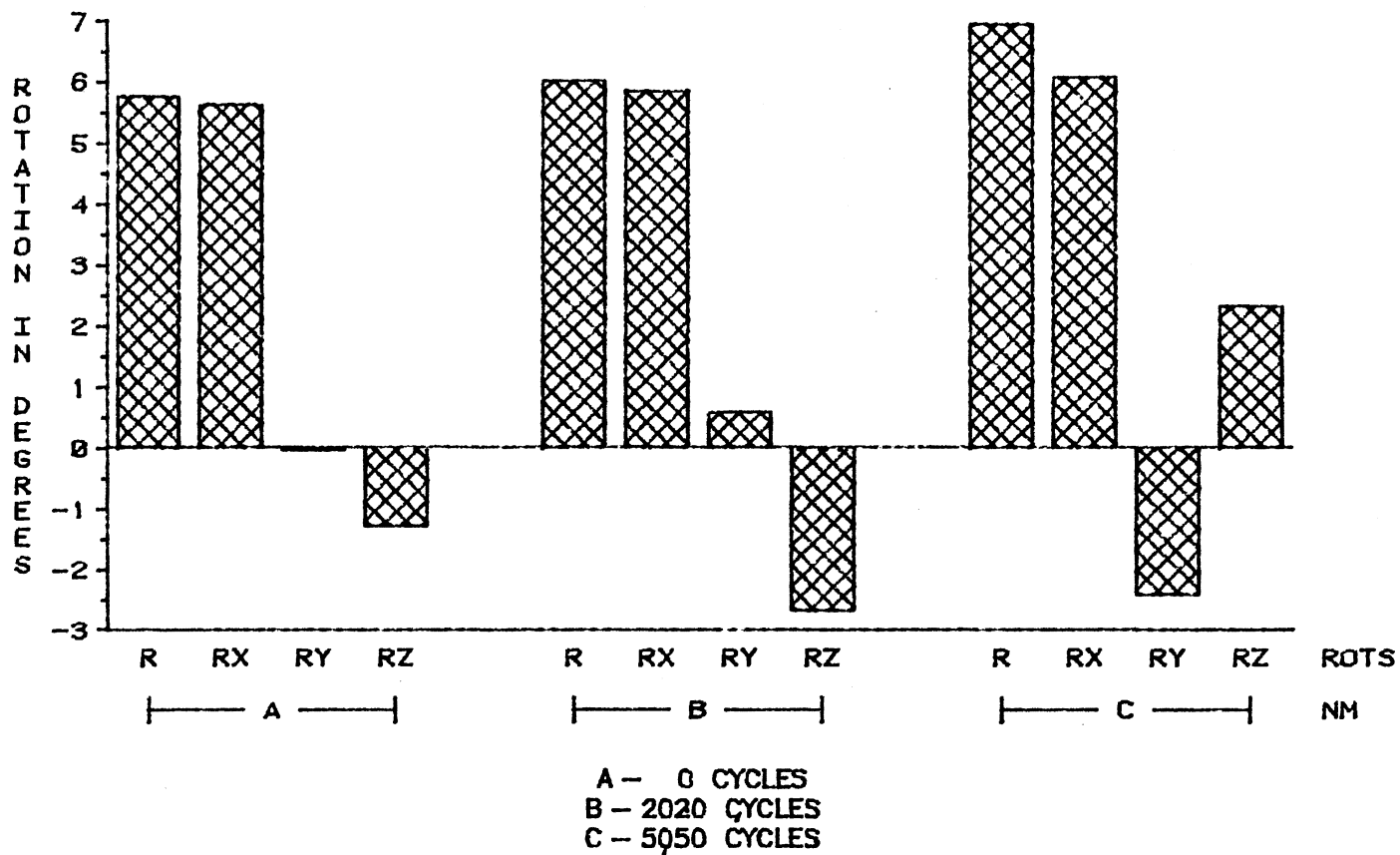
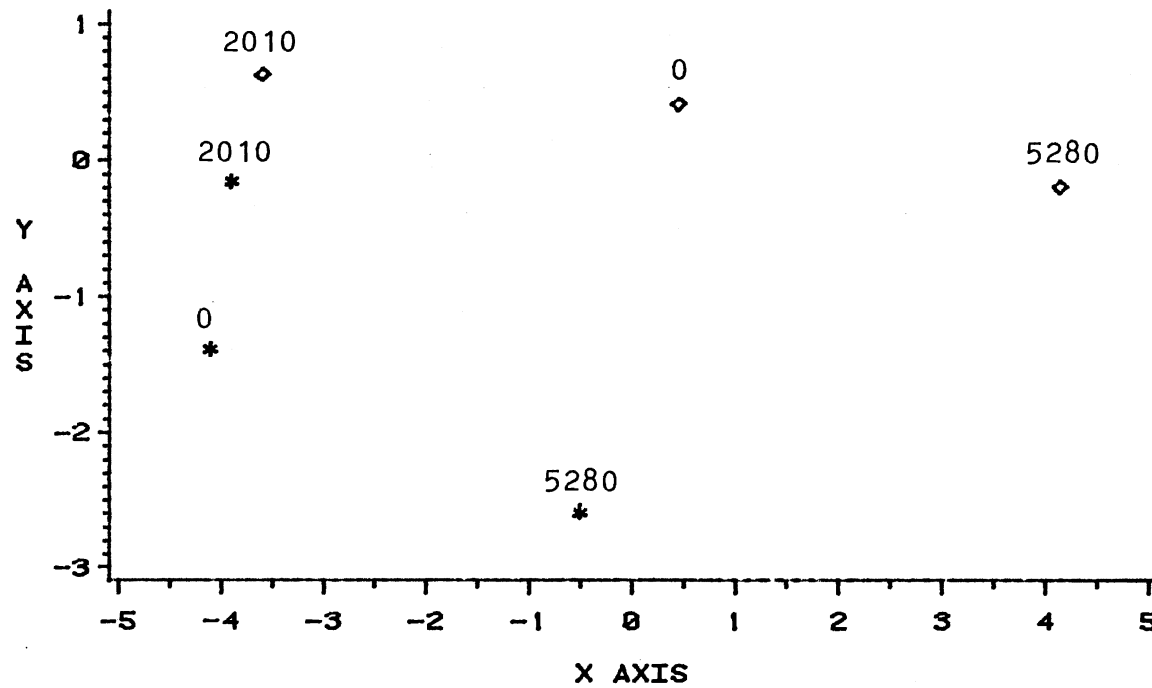


Figure 44. Rotations Under Negative Moment (90 deg.) Under Bending Fatigue Load



\* REPRESENTS POINTS FOR POSITIVE TORQUE  
 ◇ REPRESENTS POINTS FOR NEGATIVE TORQUE

Figure 45. Points of Intersection of the Screw Axis With XY Plane for PT and NT Loads Under Bending Fatigue Load

## BIBLIOGRAPHY

1. Soni, A. H., Gudavalli, M. R., Sullivan, J. A., and Herndon W. A. (1986) "Effect of Tension Preload on Lumbar Spine Kinematics and its Clinical Implication" 5th Meeting of the European Society of Biomechanics, Berlin, West Germany.
2. Soni, A. H., Gudavalli, M. R., Sullivan, J. A., and Herndon, W. A. (1986) "Role of Individual Facet Joints in the Mobility of the Lumbar Spine", Proceedings of the Annual Meeting of the International Society for the Study of the Lumbar Spine, Dallas.
3. Sullivan, J. A., Soni, A. H., Patwardhan, A. G., and Gudavalli, M. R. (1981) "Three Dimensional Range and Pattern of Intervertebral Motion in Lumbar Spine", Proceedings of the 27th Annual ORS Conference, Las Vegas, Nevada.
4. Soni, A. H., Gudavalli, M. R., and Sullivan, J. A., (1984) "Coupling Effect in Axial Loading of Lumbar Spine", Proceedings of the 37th ACEMB Meeting, Los Angeles, California.
5. Soni, A. H., Gudavalli, M. R., and Srinivasan, V., (1982) "Three Dimensional Flexibility Properties of the Lumbar Spine", Proceedings of the 35th ACEMB Conference, Philadelphia, Pennsylvania.
6. Soni, A. H., Kutubuddin, M., Garna, W. A., and Gudavalli, M.R. (1986) "Bending Fatigue Characteristics of Artificial Knee Ligaments", 5th Meeting of the European Society of Biomechanics, Berlin, West Germany.
7. Liu, Y. K., Goel, V. K., Dejong, A., Njus, G., and Nishiyama, K., and Buckwalter, J. (1985) "Torsional Fatigue of the Lumbar Intervertebral Joints", Spine, Vol. 10, No. 10, pp 894-900.
8. Koeller, W., Meier, W., and Hartmann, F., (1984) "Biomechanical Properties of Human Intervertebral Discs Subjected to Axial Dynamic Compression", Spine, Vol. 9, No. 8, pp 725-733.

9. Adams, M. A., and Hutton, W. C., (1983) "The Effect of Fatigue on the Lumbar Intervertebral Disc", J Bone and Joint Surgery, Vol. 65-B, No. 2, pp 199-203.
10. Liu, Y. K., Njus, G., Buckwalter J., and Wakano, K., (1983) "Fatigue Response of Lumbar Intervertebral Joints Under Axial Cyclic Loading", Spine, Vol. 8, No. 8, pp 857-865.
11. Nachemson, A. L., Schultz, A. B., and Berkson, M. H., (1979) "Mechanical Properties of Human Lumbar Spine Motion Segments", Spine Vol. 4, No. 1, pp 1-8.
12. Cryon, B. M., and Hutton, W. C., (1978) "The Fatigue Strength of the Lumbar Neural Arch in Spondylolysis" J Bone and Joint Surgery, Vol. 60-B, No. 2, pp 234-238.
13. Lafferty, J. F., Winter, W. G., and Gambaro, S. A., (1977) "Fatigue Characteristics of Posterior Elements of Vertebrae", J Bone and Joint Surgery, Vol. 59-A, No. 2, pp 154-158.
14. Hardy W. G., Lissner H. R., Webster J. E., et al (1958) "Repeated Loading Tests on the Lumbar Spine", Surgical Forum 9 pp 690-695.
15. Schultz, A. B., (1986) "Loads on the Human Lumbar Spine" Mechanical Engineering, Jan 1986, pp 36-41.
16. Technical Staff, Measurements Group Inc., Raleigh, NC, (1985) "Strain Gage - A Reliable Measurement Tool", Mechanical Engineering, May 1985, pp 43-47.
17. White, A. A., and Panjabi, M. M., "Clinical Biomechanics of the Spine", J. B. Lippincott Company, 1978.
18. Byars, E. F., and Snyder, R. D., "Engineering Mechanics of Deformable Bodies", Intext Educational Publishers, 1975.
19. Shigley, J. E., "Mechanical Engineering Design", Mc Graw Hill, 1977.
20. Ploakowski, N. H., Ripling, E. J., "Strength and Structure of Engineering Materials", Pretence-Hall Inc., 1966.

APPENDIX

COMPUTER PROGRAM FOR DIGITAL DATA ACQUISITION

```

( TURBO PASCAL PROGRAM WHICH USES PCLAB ROUTINES TO READ
  CONTINUOUS A/D VALUES)

PROGRAM TSTAD (INPUT, OUTPUT);

      ( ***** INCLUDE FILES ***** )

($i PCLDEFS.TP)      ( include PCLAB routine definitions )
($i PCLERRS.PAS)    ( include PCLAB error definitions )

      ( ***** DECLARATIONS ***** )

TYPE

  BIG_ARRAY = ARRAY[0..1000] OF REAL;
  REALARRAY = ARRAY[0..20] OF REAL;
  INTARRAY  = ARRAY[0..500] OF INTEGER;
  SM_INT_ARRAY = ARRAY[0..30] OF INTEGER;
  TITLE_ARRAY = ARRAY[0..50] OF STRING[40];

VAR
  VO:BIG_ARRAY;
  GAIN,NUMNEW,K,CLOCK_DIV,J,NUMREAD,NUM,ADVALUE,
      STATUS,I,CYCLES:INTEGER;
  ANS:CHAR;
  V1,V2,V3,V4,V5,V6,VOLTS,A,A0,A1,A2,A3,A4,A5,A6:REALARRAY;
  CONT:INTARRAY;
  DATA_FILE:TEXT;
  FILENAME:STRING[12];
  CD,TIME,DUM,IR,PVOLTS,PADVALUE:REAL;
  TITLE:STRING[50];
  STORE:BOOLEAN;

(-----)

PROCEDURE READ_CONTINUOUS_DATA;

BEGIN
  K := 0;

  REPEAT
    CLRSCR;
    K := K + 1;
    TEXTCOLOR(0);
    I := 0;
    WRITELN(' GAIN          BIPOLAR RANGE');

```



```

WRITELN(' 1           10 V');
WRITELN(' 10          1 V');
WRITELN(' 100         100 MV');
WRITELN(' 500           20 MV');
WRITELN;
WRITE('ENTER THE SELECTED GAIN .....');
READLN(GAIN);WRITELN;
WRITE('ENTER THE NUMBER OF CONVERSIONS.... ');
READLN(NUM);WRITELN;
WRITE('ENTER THE CLOCK DIVIDER NUMBER..... ');
READLN(CLOCK_DIV);WRITELN;
CD := CLOCK_DIV;
WRITE('ENTER THE NUMBER OF CYCLES ELAPSED..');
READLN(CYCLES);WRITELN;
WRITELN('ENTER THE DATA FILE NAME');
WRITELN('*****');
READLN(FILENAME);
CLRSCR;
TEXTCOLOR(4 + BLINK);

WRITELN('PRESS RETURN TO MAKE THE READING');READLN;
CLRSCR;
TEXTCOLOR(1);
WRITELN('TAKING READINGS....');

{ *** COMMENTS *** }

STATUS := INITIALIZE;           { initialize PCLAB routines }

STATUS := SELECTBOARD ( 1 );    { select unit1 }

STATUS := SETUPADC(0,0,0,GAIN); { setting A/D parameters }
{ arguments: timing source, start channel,
  end channel, gain }

STATUS := SETCLOCKDIVIDER(CLOCK_DIV);
{ setting the period of internal clock }

STATUS := ADCSERIES(NUM,CONT[1]);
{ arguments: number of conversions, analog data array }

STATUS := TERMINATE;           { stop the conversions }

{ *** CONVERT A/D VALUE TO VOLTAGE AND WRITE TO SCREEN *** }
CLRSCR;

NUMNEW := NUM - 1;
FOR J := 0 TO NUMNEW DO BEGIN

```

```

DUM := CONT[J];
VO[J] := (((20 * DUM / 4096) - 10)/GAIN)*1000;
WRITELN('          READING # ',J+1,' = ',CONT[J]:4,
        '          M VOLTS = ',VO[J]:5:6);

END;

( ***** STORE DATA ***** )

ASSIGN(DATA_FILE,FILENAME);
REWRITE(DATA_FILE);

WRITELN(DATA_FILE,CYCLES);

FOR I := 0 TO NUMNEW DO BEGIN
  IR := I;
  TIME := IR * CD * 2.5E-6;
  WRITELN(DATA_FILE,TIME:8:6,'          ',VO[I]:6:4);
END;
CLOSE(DATA_FILE);

WRITELN;
TEXTCOLOR(4);
WRITE('DO YOU WISH TO MAKE ANOTHER CONTINUOUS READING (Y/N)?');
READ(KBD,ANS);WRITELN;
UNTIL UPCASE(ANS) = 'N';

END; {procedure dynamic}

{-----}

PROCEDURE READ_IMMEDIATE_DATA;

BEGIN
  J:=0; NUMREAD:=0;
  REPEAT
    CLRSCR;
    WRITE('PRESS <ENTER> TO MAKE YOUR FIRST READING...');READLN;

    I := I + 1;          { ***** COMMENTS ***** }
    NUMREAD := NUMREAD + 1;

  STATUS := INITIALIZE;      { initialize PCLAB routines }

  STATUS := SELECTBOARD ( 1 );      { select board #1 }

    { the function ADCVALUE(CH,#,VAR)      }
    { reads an A/D value from channel CH, }
    { gain # and assigns to ADVALUE variable }

  STATUS := ADCVALUE(1,1,ADVALUE); { *** CHANNEL 1 *** }
  A1[I] := ADVALUE;

```

```

STATUS := ADCVALUE(2,1,ADVALUE); { *** CHANNEL 2 *** }
A2[I] := ADVALUE;

STATUS := ADCVALUE(3,1,ADVALUE); { *** CHANNEL 3 *** }
A3[I] := ADVALUE;

STATUS := ADCVALUE(4,1,ADVALUE); { *** CHANNEL 4 *** }
A4[I] := ADVALUE;

STATUS := ADCVALUE(5,1,ADVALUE); { *** CHANNEL 5 *** }
A5[I] := ADVALUE;

STATUS := ADCVALUE(6,1,ADVALUE); { *** CHANNEL 6 *** }
A6[I] := ADVALUE;

STATUS := TERMINATE;

{ ***** convert A/D values to voltages ***** }

V1[I] := (20 * A1[I]/ 4096) - 10;
V2[I] := (20 * A2[I]/ 4096) - 10;
V3[I] := (20 * A3[I]/ 4096) - 10;
V4[I] := (20 * A4[I]/ 4096) - 10;
V5[I] := (20 * A5[I]/ 4096) - 10;
V6[I] := (20 * A6[I]/ 4096) - 10;

{ NOTE: 'NUMREAD' AND 'I' ARE THE SAME }

WRITELN('READING # ',NUMREAD);WRITELN;

WRITELN(' CHANNEL 1 = ',A1[I]:5:1,' VOLTS = ',V1[I]:5:2);
WRITELN(' CHANNEL 2 = ',A2[I]:5:1,' VOLTS = ',V2[I]:5:2);
WRITELN(' CHANNEL 3 = ',A3[I]:5:1,' VOLTS = ',V3[I]:5:2);
WRITELN(' CHANNEL 4 = ',A4[I]:5:1,' VOLTS = ',V4[I]:5:2);
WRITELN(' CHANNEL 5 = ',A5[I]:5:1,' VOLTS = ',V5[I]:5:2);
WRITELN(' CHANNEL 6 = ',A6[I]:5:1,' VOLTS = ',V6[I]:5:2);
WRITELN;

WRITELN('DO YOU WISH TO STORE THE DATA IN A FILE ? (Y/N)');
READ(KBD,ANS);
IF ANS='Y' THEN STORE:=TRUE;
IF ANS='N' THEN STORE:=FALSE;

{ ***** STORE DATA ***** }

IF STORE THEN BEGIN

WRITELN('ENTER THE DATA FILE NAME');
WRITELN('*****');
READLN(FILENAME);
WRITE('ENTER THE NUMBER OF CYCLES ELAPSED...');
READLN(CYCLES);
WRITELN('ENTER THE TITLE FOR THE READING');

```

```

WRITELN('*****');
READLN(TITLE);
CLRSCR;

WRITELN('STORING DATA');
ASSIGN(DATA_FILE,FILENAME);
REWRITE(DATA_FILE);
  WRITELN(DATA_FILE,TITLE);
  WRITELN(DATA_FILE,CYCLES);
  WRITELN(DATA_FILE,V1[I]:6:4);
  WRITELN(DATA_FILE,V2[I]:6:4);
  WRITELN(DATA_FILE,V3[I]:6:4);
  WRITELN(DATA_FILE,V4[I]:6:4);
  WRITELN(DATA_FILE,V5[I]:6:4);
  WRITELN(DATA_FILE,V6[I]:6:4);

  CLOSE(DATA_FILE);
END;

WRITE('DO YOU WISH TO MAKE ANOTHER STATIC READING (Y/N)?');
READ(KBD,ANS);WRITELN;
UNTIL UPCASE(ANS) = 'N';

END; {procedure read_immediate_data}

{-----}

PROCEDURE MAIN_MENU;

BEGIN
  REPEAT
    CLRSCR;
    GOTOXY(75,50);
    TEXTCOLOR(0);
    WRITELN('          1. READ A/D CONTINUOUS, DYNAMIC');
    WRITELN;
    TEXTCOLOR(5);
    WRITELN('          2. READ A/D IMMEDIATE, STATIC');
    WRITELN;
    TEXTCOLOR(6);
    WRITELN('          3. EXIT PROGRAM');
    WRITELN;
    TEXTCOLOR(1);
    WRITE('          ENTER YOUR CHOICE (1-3)....');
    TEXTCOLOR(1);
    READ(KBD,ANS);

CASE ANS OF

  '1': BEGIN
    READ_CONTINUOUS_DATA;
    END;      { end choice #1 }

```

```
'2': BEGIN
    READ_IMMEDIATE_DATA;
    END;      { end choice #2 }

END; { case statement end }

UNTIL UPCASE(ANS) = '3';

END; { procedure end }

{-----}

{ ***** MAIN PROGRAM *****}

BEGIN
GOTOXY(50,50);
TEXTBACKGROUND(7);
  REPEAT
    MAIN_MENU;
    WRITELN('ARE YOU SURE (Y/N)');
    READ(KBD,ANS);
    UNTIL UPCASE(ANS) = 'Y';
  END.
END.
```

VITA

ENOCH MYLABATHULA

Candidate for the Degree of

Master of Science

Thesis: INFLUENCE OF FATIGUE LOADS ON THE LAXITY OF  
LUMBAR INTERVERTEBRAL JOINTS

Major Field: Mechanical Engineering

Biographical:

Personal Data: Born in Guntur, India, Aug 29, 1962,  
son of Mrs. & Mr. M. A. Prasada Rao.

Education: Recieved Bachelor of Technology degree  
in Mechanical Engineering from Jawaharlal Nehru  
Technological University, A. P., India, 1983.  
Completed requirements for Master of Science  
degree at Oklahoma State University in December  
1987.

Professional Experience: Graduate Research Assistant,  
School of Mechanical and Aerospace Engineering,  
Oklahoma State University, 1985 - 1987.